Free Radical Biology and Medicine 225 (2024) 193–207

Contents lists available at ScienceDirect

Free Radical Biology and Medicine

journal homepage: www.elsevier.com/locate/freeradbiomed

Oral administration of plumbagin is beneficial in *in vivo* models of Duchenne muscular dystrophy through control of redox signaling

Davide Cervia [a,1], Silvia Zecchini [b,1], Luca Pincigher [c], Paulina Roux-Biejat [b], Chiara Zalambani [c], Elisabetta Catalani [a], Alessandro Arcari [b], Simona Del Quondam [a], Kashi Brunetti [a], Roberta Ottria [b], Sara Casati [d], Claudia Vanetti [b,e], Maria Cristina Barbalace [f], Cecilia Prata [c], Marco Malaguti [f], Silvia Rosanna Casati [g], Laura Lociuro [f], Matteo Giovarelli [b], Emanuele Mocciaro [b,h], Sestina Falcone [i], Claudio Fenizia [b,e], Claudia Moscheni [b], Silvana Hrelia [f], Clara De Palma [g], Emilio Clementi [b,j], Cristiana Perrotta [b,*]

[a] *Department for Innovation in Biological, Agro-Food and Forest Systems (DIBAF), Università Degli Studi Della Tuscia, Viterbo, 01100, Italy*
[b] *Department of Biomedical and Clinical Sciences (DIBIC), Università Degli Studi di Milano, Milano, 20157, Italy*
[c] *Department of Pharmacy and Biotechnology (FABIT), Alma Mater Studiorum-Università di Bologna, Bologna, 40126, Italy*
[d] *Department of Biomedical, Surgical, and Dental Science (DISBIOC), Università Degli Studi di Milano, Milano, 20133, Italy*
[e] *Department of Pathophysiology and Transplantation (DEPT), Università Degli Studi di Milano, Milano, 20122, Italy*
[f] *Department for Life Quality Studies, Alma Mater Studiorum-Università di Bologna, Rimini, 47921, Italy*
[g] *Department of Medical Biotechnology and Translational Medicine (BIOMETRA), Università Degli Studi di Milano, 20054, Segrate, Italy*
[h] *Gene Expression and Muscular Dystrophy Unit, Division of Genetics and Cell Biology, IRCCS Ospedale San Raffaele, Milano, 20132, Italy*
[i] *Sorbonne Université, INSERM, Institut de Myologie, Centre de Recherche en Myologie, Paris, F-75013, France*
[j] *IRCCS Eugenio Medea, Bosisio Parini, 23842, Italy*

ARTICLE INFO

Keywords:
Duchenne muscular dystrophy
Plumbagin
Oxidative stress
Drosophila melanogaster
Mdx mice

ABSTRACT

Duchenne muscular dystrophy (DMD) is a progressive muscle-wasting disease. Recently approved molecular/gene treatments do not solve the downstream inflammation-linked pathophysiological issues such that supportive therapies are required to improve therapeutic efficacy and patients' quality of life. Over the years, a plethora of bioactive natural compounds have been used for human healthcare. Among them, plumbagin, a plant-derived analog of vitamin K3, has shown interesting potential to counteract chronic inflammation with potential therapeutic significance.

In this work we evaluated the effects of plumbagin on DMD by delivering it as an oral supplement within food to dystrophic mutant of the fruit fly *Drosophila melanogaster* and mdx mice. In both DMD models, plumbagin show no relevant adverse effect. In terms of efficacy plumbagin improved the climbing ability of the dystrophic flies and their muscle morphology also reducing oxidative stress in muscles. In mdx mice, plumbagin enhanced the running performance on the treadmill and the muscle strength along with muscle morphology. The molecular mechanism underpinning these actions was found to be the activation of nuclear factor erythroid 2-related factor 2 pathway, the re-establishment of redox homeostasis and the reduction of inflammation thus generating a more favorable environment for skeletal muscles regeneration after damage.

Our data provide evidence that food supplementation with plumbagin modulates the main, evolutionary conserved, mechanistic pathophysiological hallmarks of dystrophy, thus improving muscle function *in vivo*; the use of plumbagin as a therapeutic in humans should thus be explored further.

* Corresponding author.
E-mail address: cristiana.perrotta@unimi.it (C. Perrotta).
[1] Equal contribution.

https://doi.org/10.1016/j.freeradbiomed.2024.09.037
Received 25 July 2024; Received in revised form 12 September 2024; Accepted 23 September 2024
Available online 24 September 2024

1. Introduction

Duchenne muscular dystrophy (DMD) is the most common and severe pediatric muscular dystrophy leading to rapid loss of mobility and premature death [1]. This X-linked disease is characterized by a lethal progressive muscular-wasting, caused by mutations in the dystrophin gene that disrupt its translational reading frame or create a premature stop codon [2]. Dystrophin is a huge subsarcolemmal protein (the full-length muscle isoform, Dp427m, weights 427 kDa) with important structural and signaling functions [3]. While predominantly expressed in skeletal and cardiac muscles, it is present also in the central nervous system, including the retina, and in the skin (https://www.proteinatlas.org/ENSG00000198947-DMD). The absence of functional dystrophin reduces the stiffness of the sarcolemma and increases the susceptibility of the fibers to contraction damage. This condition triggers a cascade of events characterized by chronic inflammation and oxidative stress with an imbalance between muscle regeneration and degeneration that increases deposition of fibrotic and adipose tissue and eventually culminates in muscle loss [2,4]. The altered expression/lack of dystrophin causes also major transcriptomic and functional abnormalities in myogenic precursor cells [5].

Currently approved DMD drugs, including glucocorticoids, reduce the prolonged inflammatory response and the persistent activation of the immune system [4,6]. These drugs however must be used in patients around 4–5 years of age and their administration instead is not recommended before 2 years of age [7,8]. Noteworthy, many efforts in the last decade have led to the clinical approval of innovative therapeutic products for DMD namely readthrough small agents, exon-skipping antisense oligonucleotides, viral vectors carrying micro-dystrophin transgene, that aim to restore dystrophin expression and function; in addition to these, other therapies are currently undergoing the approval process for human use [6]. All of these approaches are selective for genetically defined subsets of patients. Moreover, the restoration of dystrophin expression with a genetic approach may be insufficient to restore the muscular deficit due to the progressive decline in muscle quality caused by chronic inflammation, redox impairment, and fibro-fatty degeneration. Combination therapies with classical pharmacological drugs and genetic therapies able to restore dystrophin expression and also target the myriad of cellular events dramatically impaired in dystrophic muscle are thus desirable. The choice of which drug could be best combined with genetic therapy rests on addressing the hallmarks of DMD muscle degeneration among which oxidative stress is a central factor [9]. Using cell and animal models of DMD, various natural products and dietary supplements, such as green tea polyphenolics, quercetin, resveratrol, curcumin, and saponins, have been found to exert protective activity, also increasing cell survival and reducing necrosis, atrophy and oxidative stress [9–12]. Due to their beneficial effects, the attention towards these compounds is rapidly increasing, with the aim of counteracting pathology-related alterations, the consequences of metabolic response to oxidative damage or modulating the immunological response of patients. Complementary and alternative medicine, along with traditional treatments, has become thus increasingly popular in DMD patients although more research into their therapeutic potential is needed [10,11,13].

Many naturally occurring molecules such as 1,4-naphthoquinones have been extensively investigated for their biological properties *in vivo* [14]. Plumbagin, 5-hydroxy-2-methyl-1, 4-naphthoquinone, is an analog of vitamin K3 originally extracted from *Plumbago zeylanica* L [15]. with a wide range of biological activities including antifungal, antibacterial, antitumor, anti-inflammatory, antioxidant, and neuroprotective effects [14,16–21]. For this reason, plumbagin has gained a lot of attention in pharmacological research due to its various potential therapeutic actions and its utilization as food-derived phytochemical compounds [22–24]. In different experimental models, plumbagin has consistently demonstrated to enhance the activity/expression of several key antioxidant enzymes (superoxide dismutase - SOD, catalase - CAT, glutathione S-transferase - GST) and Nrf2 (Nuclear factor erythroid 2-related factor 2), a pivotal transcription factor known for orchestrating the cellular antioxidant response [20,22,25–27]. Moreover, it has been demonstrated that plumbagin leads to the upregulation of glutathione (GSH) levels and enhances the activity of glutathione peroxidase (GPx) [28–30]. Therefore, plumbagin might be a promising candidate for DMD treatment, either alone or in combination with genetic therapies, although this hypothesis has not yet been tested.

Since plumbagin is usually administered as dietary supplement, in this study we have examined the biological impact of plumbagin-enriched food on the DMD skeletal muscle phenotype and the cellular/molecular events responsible of its activity. This was conducted using both the mdx mouse model of dystrophy and the fruit fly *Drosophila melanogaster* DMD model [31–34]. In these systems, plumbagin improved skeletal muscle structure and function by exerting antioxidant/anti-inflammatory effects establishing it as a therapeutic candidate with a broad mechanism of action in DMD.

2. Methods

2.1. D. melanogaster stocks, husbandry, and treatments

Dystrophic mutants used in this study were Dys^{E17}, lacking functional large-isoforms of dystrophin-like protein. Oregon-R was used as wild-type (wt) strain. All stocks were obtained from Bloomington Drosophila Stock Center (Indiana University Bloomington, IN, USA): #63047 (Dys^{E17}) and #5 (Oregon-R). Allele description of Dys^{E17}: point mutation induced by ethyl methanesulfonate on chromosome 3, 92A10, 3R:19,590,4580.19,590,458, causing a nucleotide change C19590458T and consequently the amino acid change Q2807term|Dys-PA. Third chromosome alleles were balanced with the TM6,Tb balancer chromosome.

Flies were routinely maintained and reared in the incubator at 25 °C (mild acidic pH) on a standard corn meal agar diet: 25 g of yellow cornmeal, 7 g of active dry yeast, 2 g of agar, and 27 g of sucrose (9 % w/v) were mixed and dissolved by adding warm plain water to a final volume of 300 ml, the hydration source of the flies. The mixture was autoclaved and the broad-spectrum fungicide Nipagin (0,75 g, dissolved in ethanol) was added at ca. 50 °C. Subsequently, 10 ml of cooling down mixture was dispensed into vials to reach ca. 25 °C before adding flies. All experiments were performed with female and male young adults of Drosophila of the same age. In particular, 1–3 days old flies were reared for 20 or 30 days on vials containing either the standard medium or diet supplemented with plumbagin, in agreement with previous reports [20]. Plumbagin (#M18615) was obtained from Molnova (Ann Arbor, MI, USA). Following manufacturer's protocol, dimethyl sulfoxide (DMSO) was used to prepare stock solutions of 100 mM plumbagin, stored in the dark below −20 °C to ensure its stability. The stock solution of plumbagin was diluted in water to prepare working solutions. Working solution was then mixed to food into vials at 25 °C to obtain the final concentration of plumbagin, making sure the concentration of DMSO was < 0.1 % in order to avoid poisoning effects. After a preliminary dose-response of 1 nM, 30 nM, 100 nM, and 1 μM, the final concentrations in the food used in this paper were 1 or 30 nM. Diets were renewed at day 5 to prevent the degradation of the test compound by transferring flies to a new vial containing fresh diet. Of notice, Drosophila food containing high concentrations of brewer's yeast showed considerable buffering capacity [35].

2.2. D. melanogaster survival and climbing

Fly survivorship was documented recording the numbers of dead individuals per vial every 5 days, starting at day 10 of treatment. Geotaxis was assessed every 5 days from treatment using a climbing assay (negative geotaxis reflex in opposition to the Earth's gravity). *D. melanogaster* were separated into cohorts (empty vials) consisting of

ca. 20 flies. A horizontal line was drawn 15 cm above the bottom of the vial. After a 10 min rest period, the flies were tapped to the bottom of the vials: all flies were forced to start climbing (vertical walking). The number of flies that climbed up to the 15 cm mark after 60 s was recorded as the percentage success rate. A camera was recording fly movement during the experiment. Each trial was performed three times, at 1 min intervals, and the results were averaged.

2.3. Fluorescence microscopy in D. melanogaster

Drosophila thoraxes were collected and immersion-fixed overnight in cold 4 % paraformaldehyde in 0.1 M Phosphate Buffer (PB) at 4 °C. Samples were then transferred to cold 15 % sucrose in PB and stored at 4 °C for at least 48 h. Longitudinal sections of thorax muscles, *i.e.* dorsal longitudinal muscle (DLM) (16 μm) were obtained by a cryostat, mounted onto positive charged slides, and stored at −25 °C until use. To ensure accurate comparison, the same depth/region of the structure was analyzed.

To observe Drosophila muscle structure, sections were incubated for 24 h at 4 °C with phalloidin-iFluor 555 reagent (#ab176756, Abcam, Cambridge, United Kingdom). For immunostaining detection, muscle sections were pre-incubated for 30 min at room temperature with 5 % BSA and 10 % of normal goat serum in PB containing 0.5 % Triton X-100. Pre-treated sections were then incubated overnight at 4 °C with anti-nitrotyrosine rabbit primary antibody (Invitrogen-ThermoFisher Scientific, Monza, Italy) (Supplementary Table 1) in PB containing 0.5 % Triton X-100. Following washes in PB, the sections were incubated in the Alexa Fluor goat anti-rabbit 546 secondary antibody in PB overnight at room temperature. The slides were coverslipped with Fluoroshield Mounting Medium containing DAPI (Abcam) for nuclei detection. Incubation in secondary antibody alone was routinely performed as a negative control. Images were acquired by a Zeiss LSM 710 confocal microscope and the distance between adjacent focal planes (z-stacks) was set at 1 μm. The analysis of thorax muscle lesions (number of degenerated areas) or nitrotyrosine immunostaining (fluorescence levels) was carried out on two muscle sections for each animal (at least two images for sections) [33]. Fluorescence levels were quantified using ImageJ software (NIH, USA).

2.4. Mice and treatment

Male mdx (C57BL/10ScSn-Dmdmdx/J) and wt (C57BL/10ScSnJ) mice were housed in a pathogen-free facility in an environmentally controlled room (23 °C ± 1 °C, 50 % ± 5 % humidity) with a 12-h light/dark cycle and provided food and water ad libitum. All procedures were carried out in strict accordance with the Italian law on animal care (D.L. 26/2014, implementation of the 2010/63/UE) and approved by the University of Milan Animal Welfare Body and by the Italian Minister of Health (protocol n. 19/2021-PR). All efforts were made to reduce both animal suffering and the number of animals used. The experimental procedures used respected the standard operating procedures for preclinical tests in mdx mice available on https://www.treat-nmd.org/resources-and-support/sop-library/mdx-mouse-dmd/.

Plumbagin (250 mg/kg) and quercetin (400 mg/kg; Sigma-Aldrich) were dissolved in the diet (Mucedola, Milano, Italy) and administered orally, starting at 1 month of age for 3 months. The diet was added weekly and its consumption, as a measure of drug intake, was assessed by weighting it weekly before the next diet administration. N-acetylcysteine (NAC; Sigma-Aldrich) was dissolved in the drinking water (1 %). To ensure drug stability, the water was changed three times a week. The control mdx mice received the same diet and the water without any drug added. Body weight and food intake were monitored weekly for 3 months. At the end of the treatment blood was collected from the retro-orbital sinus and serum was prepared for further analysis.

2.5. Liquid chromatography tandem mass spectrometry

Plumbagin was quantified in mice serum samples by Liquid chromatography tandem mass spectrometry (LC-MS/MS) on a 1290 Infinity ultra-high-performance liquid chromatography system coupled to a Q Trap 5500 linear ion trap triple quadrupole mass spectrometer operating in multiple reaction monitoring (MRM) mode and equipped with an electrospray ionization (ESI) source as described in supplementary data. Total plumbagin was extracted and quantified after hydrolysis performed in presence of the β-glucuronidase enzyme at 37 °C and overnight. Briefly, an aliquot of serum sample (200 μl) was spiked with internal standard (plumbagin-d3), a buffer solution at pH 6.8 was added and the extraction was performed with n-butyl chloride. The organic layer was drayed and reconstituted in 50 μl of methanol and 10 μl aliquot was analyzed (Supplementary information and Supplementary Table 2).

2.6. Whole body tension test

The whole body tension (WBT) test was used to determine the ability of mice to exert tension in a forward pulling maneuver that is elicited by stroking the tail of the mice in accordance with the SOP of TREAT-NMD (http://www.treatnmd.eu/downloads/file/sops/dmd/MDX/dmd_m.2.2.006.pdf).

The tails were connected to an MP150 System transducer (BIOPAC Systems, Goleta, CA, USA) with a metal thread (one end of the thread being tied to the tail and the other end to the transducer). Mice were placed into a small tube containing a metal screen with a grid spacing of 2 mm. Forward pulling movements were elicited by tail pinches with serrated forceps and the corresponding tensions were recorded using the AcqKnowledge software recording system (BIOPAC Systems). Between 20 and 30 pulling tensions were recorded during each session. The WBT was determined by dividing the average of the top five (WBT5) or top ten (WBT10) tensions recorded by the body weight and represent the maximum phasic tension that can be developed over several attempts [36,37]. The recovery score is an index that provides the effect of drug treatments on a given parameter and was calculated according to Standard Operating Procedures (SOPs) described in the TREAT-NMD website (http://www.treat-nmd.eu/research/preclinical/dmd-sops/) as follows: Recovery score = [mdx treated]−[mdx untreated]/[wild type]−[mdx untreated] × 100.

2.7. Exhaustion treadmill test

Mice were made to run on the standard treadmill machine Exer 3/6 Treadmill (Colombus Instruments, Columbus, OH, USA) horizontally to assess their resistance to fatigue following the TREAT-NMD SOP (http://www.treatnmd.eu/downloads/file/sops/dmd/MDX/DMD_M.2.1.003.pdf). The exhaustion treadmill test was performed after an appropriate acclimatization period consisting of three sessions at 8 cm/s for 5 min. The test consisted of an initial run at 5 min at 8 cm/s, then the speed was increased by 2 cm/s every minute until reaching either 50 cm/s or exhaustion. The criterion for exhaustion was determined as the inability of the mouse to return to run within 10 s after direct contact with the electric stimulus grid. The software provided the time and the speed of the running, from which the distance run by each mouse was calculated [36]. The recovery score was calculated as for the WBT test.

2.8. RNA extraction and PCR

The mRNA expression evaluation in Drosophila and mice muscles was performed as previously described [38–42]. Total RNA was isolated by phase separation in PureZOL reagent (Bio-Rad) according to the manufacturer's protocol. Total RNA, solubilized in RNase-free water was quantified by Nanodrop 2000 spectrophotometer (ThermoFisher, Walthan, MA, USA) and retro-transcribed (800–1000 μg) using iScript

gDNA Clear cDNA Synthesis Kit (Bio-Rad). Quantitative PCR (RT-qPCR) was performed using SsoAdvanced™ Universal SYBR Green Supermix (Bio-Rad) and the CFX96 Touch Real-Time PCR Detection System (Bio-Rad). The primers pairs (Bio-Fab Research, Roma and Eurofins, Milano, Italy) are detailed in the Supplementary Tables 3 and 4. RPL32 (Drosophila) and RPL32/RPL38/36B4/GADPH (mouse) have been used as housekeeping genes for normalization by using the $2^{-\Delta\Delta CT}$ method.

2.9. Histology and immunofluorescence of mouse skeletal muscle

Muscles were dissected, frozen in liquid nitrogen-cooled isopentane and cut in serial 7 μm thick sections cut with a cryostat. Hematoxylin-eosin (H&E, Bio Optica, Milan, Italy), Picrosirius Red staining (Sigma-Aldrich) and immunofluorescence were performed as previously described [37,43]. For immunofluorescence, sections were fixed for 10 min with 4 % paraformaldehyde (PFA) in PBS and then blocked with PBS added with 10 % normal goat serum and 0.1 % Triton X-100 for 1h. The primary antibodies and the appropriate fluorescent-labeled secondary antibodies, diluted in blocking solution, were incubated overnight at 4 °C and for 1h at room temperature, respectively. Nuclei were counterstained with DAPI (PureBlu, Bio-Rab) before mounting the slides with the Fluoroshield Histology Mounting Medium (Sigma-Aldrich). The primary antibodies used were: Laminin A (Sigma-Aldrich), embryonal myosin heavy chain (MyHC-Emb; Santa Cruz Biotechnology, Dallas, TX, USA), Myozenin-1 (Sigma-Aldrich), CD45 (Miltenyi Biotec, Bergisch Gladbach, Germany) (Supplementary Table 1). To evaluate muscle damage, after fixation and blocking, sections were directly incubated with a rabbit anti-mouse IgG conjugated to Alexa Fluor® (ThermoFisher) for 1 h, counterstained with DAPI, and mounted. Images were acquired using a DMI4000 B fluorescence microscope Leica automated inverted microscope equipped with a DCF310 digital camera (Leica Microsystems, Wetzlar, Germany) or the ZOE™ Fluorescent Cell imager (Bio-Rad) and the Leica TCS SP8 System equipped with Leica DMi8 inverted microscope, for confocal imaging. Image analysis was performed by using ImageJ software.

2.10. Flow cytometry

Hind limb skeletal muscles of mice were harvested, minced and digested in a solution of Dispase and type II collagenase diluted in DMEM at 37 °C for 40 min. Disaggregation was stopped with 20 % FBS and cells were filtered through a 70 μm cell strainer (Miltenyi Biotec). The collected cells were washed with PBS and incubated with primary conjugated antibodies for 15 min at room temperature. Satellite cells were identified as an enriched population of α7-Integrin-PE (AbLab, Vancouver, BC, Canada) and CD34-Allophycocyanin Alexa Fluor 700 (APC-A700) (BD Pharmingen, San Diego, CA, USA) double-positive cells and CD45-PE-Cy7, CD31-PE-Cy7, CD14-FITC (eBioscience, San Diego, CA, USA) and Sca1-FITC (BD Pharmingen) negative cells (Supplementary Fig. 1 and Supplementary Table 1) [37]. M1 macrophages were identified as CD45-PE-Cy7 (eBioscience), F4/80-PE (Miltenyi Biotec), CD80-FITC (eBioscience) positive cells and CD206-AF647 (Sony Biotechnology) negative; M2 macrophages as CD45-PE-Cy7 (eBioscience), F4/80-PE (Biolegend), CD206-AF647 (Sony Biotechnology) positive cells and CD80-FITC (eBioscience) negative cells [37] (Supplementary Fig. 2 and Supplementary Table 1) [37]. Samples were acquired by using CytoFLEX™ flow cytometer system equipped with CytExpert software (Beckman Coulter). Data were analyzed using Kaluza software, version 2.1.1 (Beckman Coulter).

2.11. Western blotting

Mice muscles were homogenized by Ultra-Turrax (Ika-lab, Staufen, Germany) in lysis buffer containing 20 mM Tris-HCl (pH 7.4), 10 mM EGTA, 150 mM NaCl, 1 % Triton X-100, 10 % glycerol, SDS 1 % supplemented with a cocktail of protease and phosphatase inhibitors (cOmplete and PhosSTOP; Roche Applied Science Mannheim, Germany). After centrifugation at 10,000g for 10 min, total protein concentration was measured using the Bradford Protein Assay Kit (DC Protein Assay; Bio-Rad), according to the manufacturer's instruction [44]. Protein samples (10 μg) were separated on Mini-PROTEAN® TGX Stain Free™ 4–15 % Gels (Bio-Rad) in Tris–glycine buffer using electrophoresis at 150 V for 60 min and then transferred to a nitrocellulose membrane. At the Membranes were blocked in Tris-buffered saline with 5 % BSA for 1 h at room temperature and incubated with primary antibodies rabbit Nrf2 (Cell Signaling Technology, Danvers, Massachusetts, USA), HO-1 (Cell Signaling Technology), GPx1 (BIOS), SOD3 (AbClonal, Dusseldorf, Germany) overnight at 4 °C (Supplementary Table 1). Membranes were washed 3 times in Tris Buffered Saline buffer + Tween 0,05 % and incubated with peroxidase-conjugated anti-rabbit secondary antibody (Cell Signaling Technology) for 1 h at room temperature. Bands in the membranes and stain-free gels were visualized using the Chemidoc MP Imaging System (Bio-Rad). Densitometric analysis was performed with ImageLab software (Bio-Rad) and bands were normalized on the he respective loading control (total amount of protein loaded).

2.12. Statistical analyses

Due to ethical concerns, the fewest vertebrate animals possible were used to obtain valid scientific results; therefore 5–8 mice were used for each experimental group and analytical method. This was not applied in Drosophila experiments. Statistical significance of raw data between the groups was evaluated using unpaired (independent samples) Student's t-test or one-way ANOVA followed by Bonferroni or Tukey post-tests (multiple comparisons). When data were not normally distributed, the Mann-Whitney test was used. The results are expressed as means ± SEM of the indicated n values. p values ≤ 0.05 were considered statistically significant. The analysis was carried out by using the version 10.2.3 of GraphPad Prism software package (GraphPad Software, San Diego, CA, USA).

3. Results

3.1. Plumbagin ameliorates muscle function and structure in dystrophic Drosophila

Drosophila *dys* is as complex as its mammalian counterparts since encodes three large-isoforms of dystrophin-like protein (DLP1, DLP2, and DLP3) and three truncated products (Dp186, Dp205 and Dp117) [45]. Since *dys* gene is evolutionarily well conserved, we used a genetic loss-of-function homozygous mutant for *dys*, *i.e.* Dys^{E17}, as a fly model of DMD [46] to preliminarily evaluate plumbagin effects *in vivo*. Dys^{E17} is a null allele because of a nonsense mutation, that truncates the protein just before the WW domain mediating the interaction between dystrophin and dystroglycan.

A preliminary dose-response, *i.e.* 1 nM, 30 nM, 100 nM, and 1 μM of diet-supplemented plumbagin was tested for 30 days, evaluating the general behavior of adult flies and their survival rate. In both wt and Dys^{E17} strain, micromolar and submicromolar concentrations of plumbagin appeared toxic at visual observations and significantly decreased the viability of Drosophila while 1–30 nM plumbagin had no effects when compared with controls (Fig. 1A). Therefore, subsequent experiments were performed by adding plumbagin in food at a final concentration of 1 or 30 nM.

To assess whether plumbagin plays a role in reversing muscle impairment of dystrophic Drosophila, we first analyzed the mobility of flies by measuring their climbing capability. The rate of climbing decay in Dys^{E17} mutants was faster than that observed for wt and recovered, at least in part, in the presence of 1 nM plumbagin (Fig. 1B). The climbing decay of Dys^{E17} + 30 nM plumbagin was superimposable to that in wt ($T_{1/2}$ mobility: wt 25.7 days, Dys^{E17} 14.3 days, Dys^{E17} + 1 nM plumbagin

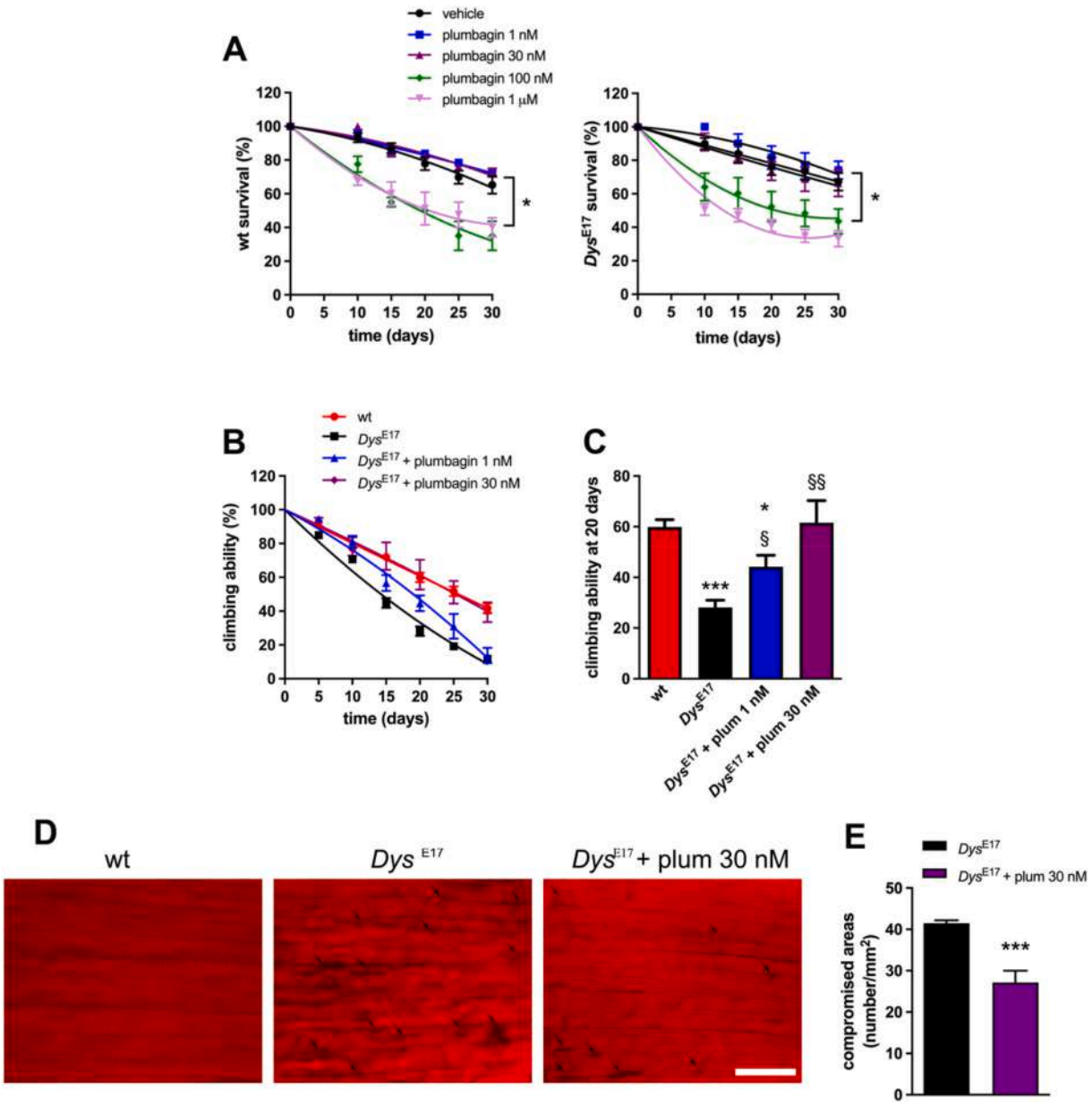

Fig. 1. ***Effects of plumbagin in Drosophila.*** Eclosed fly adults were raised in the absence and in the presence of different concentrations of plumbagin in the food. (A) Survival rate in wt (right panel) and *Dys*^{E17} (left panel) evaluated by counting the total number of living flies during the experimental period. Results are expressed as a percentage of animals at day 0. Data have been obtained from at least 4 independent experiments (80 animals). *$p < 0.01$ vs. vehicle. (B) Curve fit analysis of climbing ability at different time-points of wt, *Dys*^{E17}, and *Dys*^{E17} + plumbagin 1 or 30 nM. The number of flies that climbed up to the 15 cm mark at 60 s was recorded every 5 days. Results are expressed as success rate percentage of animals at day 0. The lower panel depicts the 50 % climbing decay ($T_{1/2}$ mobility), i.e. the day on which 50 % of animals have reduced mobility. (C) Climbing ability of wt, *Dys*^{E17}, and *Dys*^{E17} + plumbagin 1 or 30 nM on day 20 of treatment. Data have been obtained from at least 9 independent experiments (180 animals). *$p < 0.01$ and ***$p < 0.0001$ vs. wt; §$p < 0.01$ and §§$p < 0.001$ vs. *Dys*^{E17}. (D) Confocal microscopy analysis of longitudinal sections of DLM muscles stained with the F-actin fluorescent marker phalloidin in wt, *Dys*^{E17}, and *Dys*^{E17} + plumbagin 30 nM on day 20 of treatment. Black arrows indicate the most evident degenerated areas. Scale bar = 20 μm. (E) Quantitative analysis of muscle lesions. Results are expressed as the average number of the degenerated areas in a square millimeter. Images and data are representative of at least 11 animals obtained from 3 independent experiments. ***$p < 0.0001$ vs. *Dys*^{E17}.

19.1 days, *Dys*^{E17} + 30 nM plumbagin 25.4 days). Of interest, the climbing ability of *Dys*^{E17} at 20 days was *c.a.* 55 % lower vs. wt and becomes progressively higher as the concentration of plumbagin increases until reaching wt in the presence of 30 nM of the compound (Fig. 1C).

To understand the cell biological basis for the observed mobility effects of Drosophila, we analyzed the morphology of DLM at 20 days. Fluorescent phalloidin staining to visualize actin striations in longitudinal sections showed extensive degeneration of *Dys*^{E17} muscle (Fig. 1D). DLM appeared less organized than wt and numerous lesions were observed. Treatment with 30 nM plumbagin restored partially the muscle structure of the thorax and significantly reduced the number of compromised areas (Fig. 1E).

3.2. *Plumbagin treatment is safe and improves muscular structure, regeneration, and function in mdx mice*

The results obtained in flies prompted us to evaluate plumbagin in

mdx mice. Based on the daily food intake measured for mdx mice, a diet containing plumbagin was prepared at the concentration of 250 mg/kg, such that they received an effective dose of the compound (*c.a.* 30 mg/kg/day) [47,48] (Table 1). The period of treatment started when the mice were 1 month old and lasted for 3 months (Fig. 2A). Plumbagin did not affect the food and water intake and consequently did not alter the weight gain of the animals (Table 1 and Fig. 2B). At the end of the treatment, plumbagin, measured in the blood serum of the mdx mice treated with it, was 14.31 ± 2.39 ng/ml (Fig. 2C). We also assessed the effect of plumbagin on the morphology of skeletal muscle. The analysis of the diaphragms obtained from the vehicle-treated group (mdx vehicle, control) showed a muscle degeneration, with the appearance of damaged and necrotic fibers (Fig. 2D–G) accompanied by frequent foci of fibrosis as revealed by the Sirius Red staining (Fig. 2H–I). Plumbagin treatment (mdx plumbagin group) yielded an improved, nearly normal, architecture of the muscle with significant reduction of muscle damage (Fig. 2D–E), myonecrosis (Fig. 2F–G) and fibrosis (Fig. 2H–I) compared to the vehicle-treated mdx mice. The positive effect of plumbagin on membrane integrity of skeletal muscles of mdx mice was confirmed by the decrease of creatin kinase (CK) activity serum levels, as a proxy of membrane muscle damage (Supplementary Fig. 3).

Under dystrophic conditions, the regenerative capacity of the muscle is impaired such that physiological repair cannot effectively compensate for damage [49]. Plumbagin administration to mdx mice ameliorated diaphragm muscle regeneration as revealed by: i) the positivity to embryonic myosin heavy chain (MyHC-emb) identifying regenerating fibers and the significant higher expression of myozenin1 (Myoz1), a marker of regenerated fiber maturity [37,50] (Fig. 3A–D) and ii) the increased mRNA levels of transcription factors fundamental for myogenesis, such as Myf5 and MyoD (Fig. 3E). The fact that MyHC-emb signal in plumbagin-treated group was not significantly higher than control confirmed that fiber regeneration is already high in mdx mice but that plumbagin enhanced fibers maturation (Myoz1 positive fibers). Moreover, analyzing the hind limb muscles we also found in the plumbagin-treated mdx group vs. controls a significantly higher percentage of satellite cells, the stem cells of adult muscle (Fig. 4A), as well as higher expression levels of the transcription factors Myf5, MyoD, Myogenin and MRF4, assessed in the tibialis anterior muscles (Fig. 4B). The mRNA for the Insulin-like growth factor-1 (IGF-1), which potentiates skeletal muscle regeneration via activation of satellite cells [51] was also significantly upregulated in both diaphragm and tibialis anterior of mdx-treated group when compared to the control (Figs. 3E and 4B).

The structural muscle improvement by plumbagin was accompanied by the recovery of muscle function, as assessed by the whole body tension (WBT) and the treadmill until exhaustion tests at the end of the period of treatment (3 months).

As controls to assess the effectiveness of plumbagin, two additional groups of mice were included in the study, one treated with NAC (around 1 % in the drinking water) and the other with quercetin (400 mg/kg in the diet), two compounds with well-known antioxidant properties already tested in mdx mice [52–56]. As shown in Fig. 4C, plumbagin significantly improved muscle force compared with the vehicle-treated mdx mice (recovery score vs. the vehicle-treated wt mice: WBT5 = 79.97 %; WBT10 = 61.24 %) in a way similar to NAC; instead, quercetin did not display any effect. Moreover, diet supplementation with plumbagin increased the time to reach the exhaustion and the distance run by the mdx mice at the same extent as the other two compounds (Fig. 4D–E), with a recovery score of 63.50 % and 26,53 % vs. the vehicle-treated wt mice, respectively.

Table 1
Mean daily food and water intake per animal during the period of treatment (n ≥ 6 mice per group).

	vehicle	plumbagin
Daily food intake (g; mean ± SD)	4.087 ± 0.2589	3.945 ± 0.2831
Daily water intake (ml; mean ± SD)	4.205 ± 0.5559	3.947 ± 0.3964

3.3. Plumbagin mitigates oxidative stress and reduces inflammation in dystrophic muscles

We then decided to deeply investigate the effect of plumbagin on dystrophic muscles, focusing on its antioxidant/anti-inflammatory activities from a biochemical perspective. The reason why we decided to study the role in redox signaling is twofold: the well-known inhibitory activity of plumbagin on NOX4, one of the most important ROS sources (therefore, an antioxidant mechanism different from the direct scavenger of ROS), and plumbagin action as a modulator of the transcription Nrf2, a master regulator in protecting cells and tissues from oxidative stress and inflammation [20,57–60]. As reported in Fig. 5A–C, the long-term treatment (3 months) with plumbagin significantly enhanced the expression of Nrf2 and its downstream target genes Heme oxygenase-1 (HO-1), Glutathione peroxidase 1 (GPX1) and Superoxide dismutase 3 (SOD3) in the muscle of mdx mice.

The muscular antioxidant effects of food supplemented with plumbagin (30 nM, 20 days) were then verified in the Drosophila DMD model. We detected higher levels of peroxynitrite, as labeled by nitrotyrosine antibody, in DLM of dystrophic flies when compared with wt, while the signal decreased in Dys^{E17} + 30 nM plumbagin group (Fig. 5D). Specifically, treatment with plumbagin significantly decreased the nitrotyrosine fluorescent aggregates of Dys^{E17} DLM (Fig. 5E), indicating lower levels of ROS. To further test this issue, the mRNA expression of conserved prototypical (oxidative) stress response genes was assessed in extracts of Drosophila Dys^{E17} thoraxes. As shown in Fig. 5F, treatment with plumbagin significantly increased transcript levels of superoxide dismutase SOD1 and 2, catalase (CAT), and glutathione-S-transferase (GstD1). In addition, the mRNA for cap 'n' collar isoform C (CncC) gene, the homolog of the mammalian Nrf2 [61], was upregulated in the presence of plumbagin.

Finally, we investigated whether plumbagin-induced modulation of redox status may parallel with anti-inflammatory effects in dystrophic skeletal muscles. Mdx mice treated with plumbagin for 3 months showed an overall lower immune infiltrate in diaphragm muscle sections than in the vehicle treated mdx mice, as determined by the reduced areas immune-positive for CD45 (a marker of inflammatory cells) (Fig. 6A–B). This reduced inflammatory state was accompanied by an increased expression of the anti-inflammatory cytokines IL4 and IL10 (Fig. 6C), and the decreased expression of the pro-inflammatory TNF-alpha; no variations were observed for IL1beta. These data were confirmed further in the tibialis anterior muscle (Fig. 6D).

Macrophages are among the main actors in the regulation of the inflammatory process in the dystrophic muscles, with the pro-inflammatory M1 cells worsening muscle damage while the anti-inflammatory M2 cells promoting tissue repair [62,63]. We evaluated the relative presence of M1 and M2 differentiated macrophages as well as the mRNA levels of well-known M1 and M2 markers. Flow cytometry analysis in hind limb muscles of mdx mice treated with plumbagin revealed a significant decrease of the M1/M2 ratio vs. controls (Fig. 6E). Accordingly, increased expression of the M2 markers CD206, CD163 and arginase was found in the diaphragm and tibialis anterior dystrophic muscles after treatment with plumbagin, while the level of the M1 marker iNOS was unaffected (Fig. 6F–G).

4. Discussion

In this study, we investigated thoroughly the oral administration of the natural plant extract plumbagin, known for its antioxidant activities in systems other than muscle, for potential therapeutic benefit in DMD. We used two relevant models of the disease, the *D. melanogaster* Dys^{E17} and the mdx mice. Both models have been previously used in parallel to explore pathophysiological aspects and evolutionary conserved molecular mechanisms during skeletal muscle injury and also in the absence of

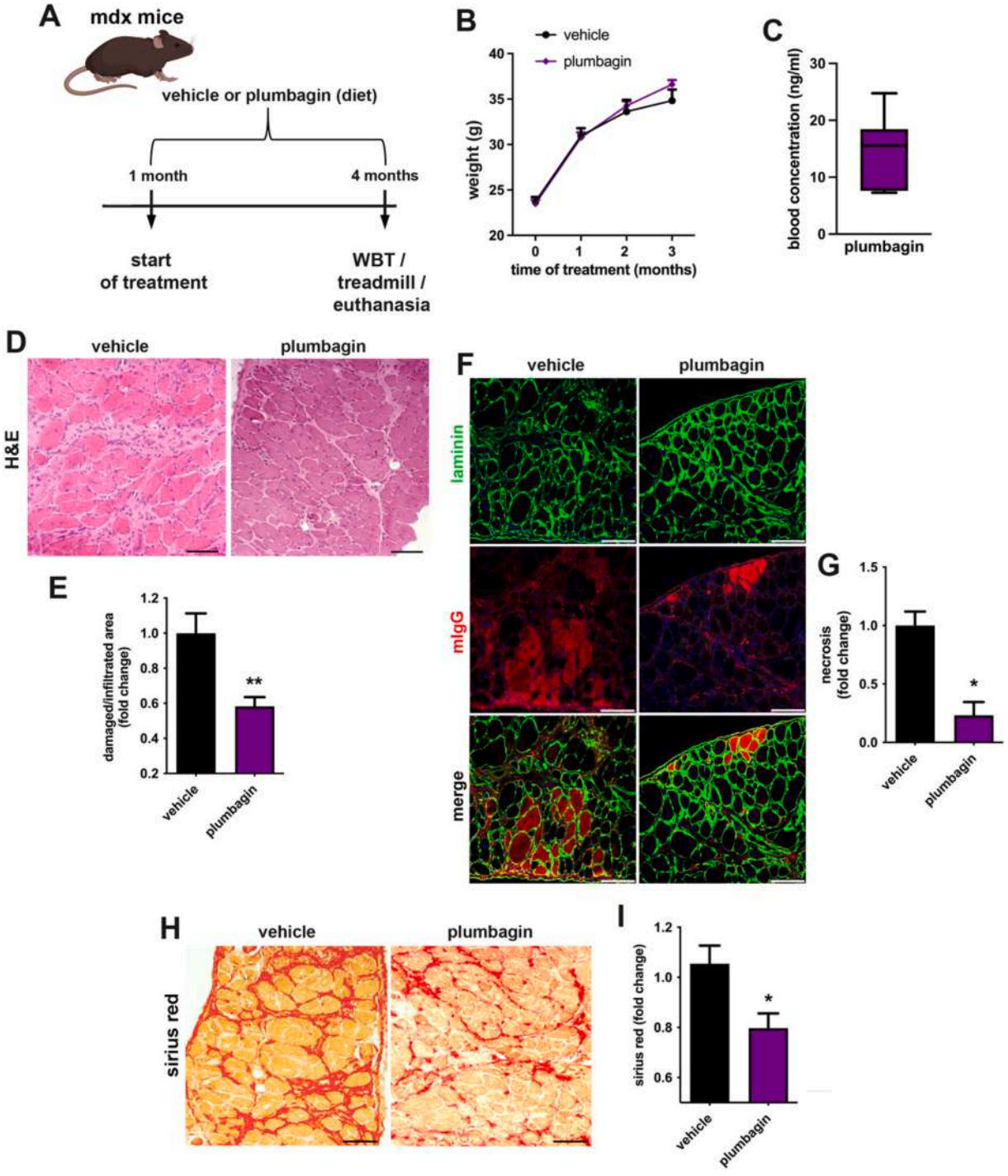

Fig. 2. ***Effects of plumbagin on murine dystrophic muscles.*** (A) Scheme of plumbagin treatment of 1 month old mdx mice. Plumbagin was administered orally in the diet (dosage: *c.a.* 30 mg/kg/day) for three months. At the end of the treatment, muscle force was measured by the WBT test and muscle performance was also evaluated by treadmill test. Then, mice were sacrificed for muscle collection and analysis. (B) Growth curves of mdx mice, measured by assessing the body weight during the period of treatment ($n \geq 6$ mice per group). (C) Quantification of plumbagin in serum by LC-MS/MS at the end of the treatment with plumbagin ($n = 7$ mice). (D) Representative images of H&E staining of diaphragm (scale bar = 100 μm) of mdx mice treated with vehicle or plumbagin. (E) The graph shows the quantification of the damaged/infiltrated areas. Values are expressed as fold change compared to the vehicle (mean ± SEM; $n \geq 5$ mice per group; $^{**}p < 0.01$ vs. vehicle). (F) Representative images of mouse IgG staining (red) of damaged fibers (scale bar = 100 μm) of diaphragms of mdx mice treated with vehicle or plumbagin. Laminin (green) was used as sarcolemma marker to identify fiber; nuclei were stained with DAPI (blue). (G) Quantification of the necrotic areas. Values are expressed as fold change compared to the vehicle (mean ± SEM; $n \geq 3$ mice per group; $^{*}p < 0.05$ vs. vehicle). (H) Representative images of Picrosirius Red staining of the collagen deposition (scale bar = 100 μm) of diaphragm of mdx treated with vehicle or plumbagin. (I) Quantification of collagen deposition expressed as fold change compared to the vehicle (mean ± SEM; $n = 5$ mice per group; $^{*}p < 0.05$ vs. vehicle).

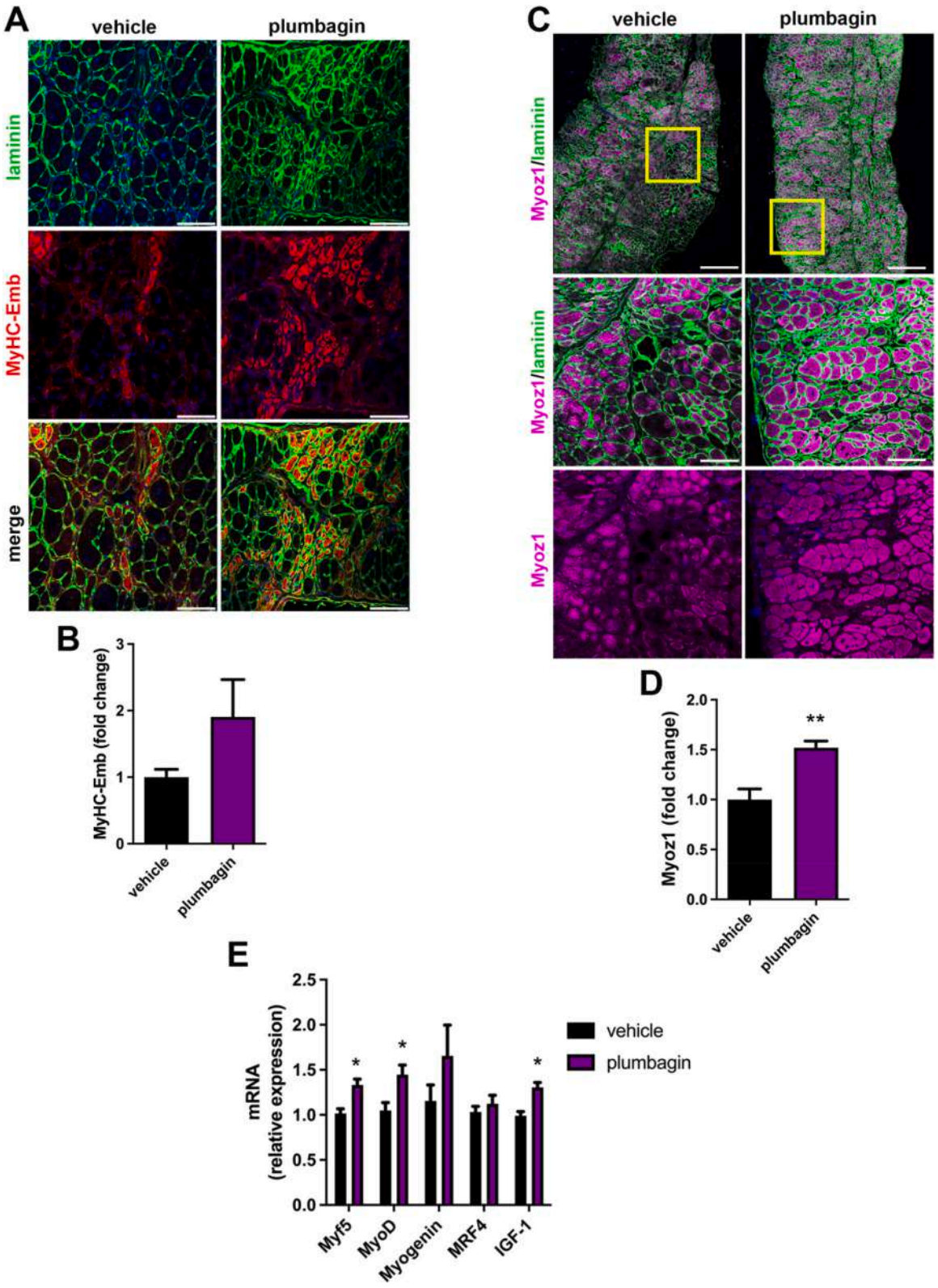

Fig. 3. ***Effect of plumbagin on muscle regeneration of mdx mice.*** (A) Representative images of embryonic myosin heavy chain (MyHC-emb) staining identifying regenerating fibers (scale bar = 100 μm) of diaphragm of mdx mice treated with vehicle or plumbagin. Laminin (green) was used as sarcolemma marker to identify fiber; nuclei were stained with DAPI (blue). (B) Quantification of areas positive to MyHC-emb. Values are expressed as fold change compared to the vehicle (mean ± SEM; n = 3 mice per group). (C) Representative images of Myoz1 staining identifying mature regenerating fibers (upper panel, scale bar = 300 μm; lower panels, scale bar = 100 μm) of diaphragm of mdx mice treated with vehicle or plumbagin. Laminin (green) was used as sarcolemma marker to identify fiber. (D) Quantification of areas positive to Myoz1. Values are expressed as fold change compared to the vehicle (mean ± SEM; n = 4 mice per group). **$p < 0.01$ vs. vehicle. (E) RT-qPCR analysis of myogenic markers Myf5, MyoD, Myogenin, MRF4 and IGF-1 of diaphragm of mdx mice treated with vehicle or plumbagin. Values are expressed as mean ± SEM (n ≥ 5 mice) normalized vs. the vehicle treated mice. *$p < 0.05$, vs. the vehicle.

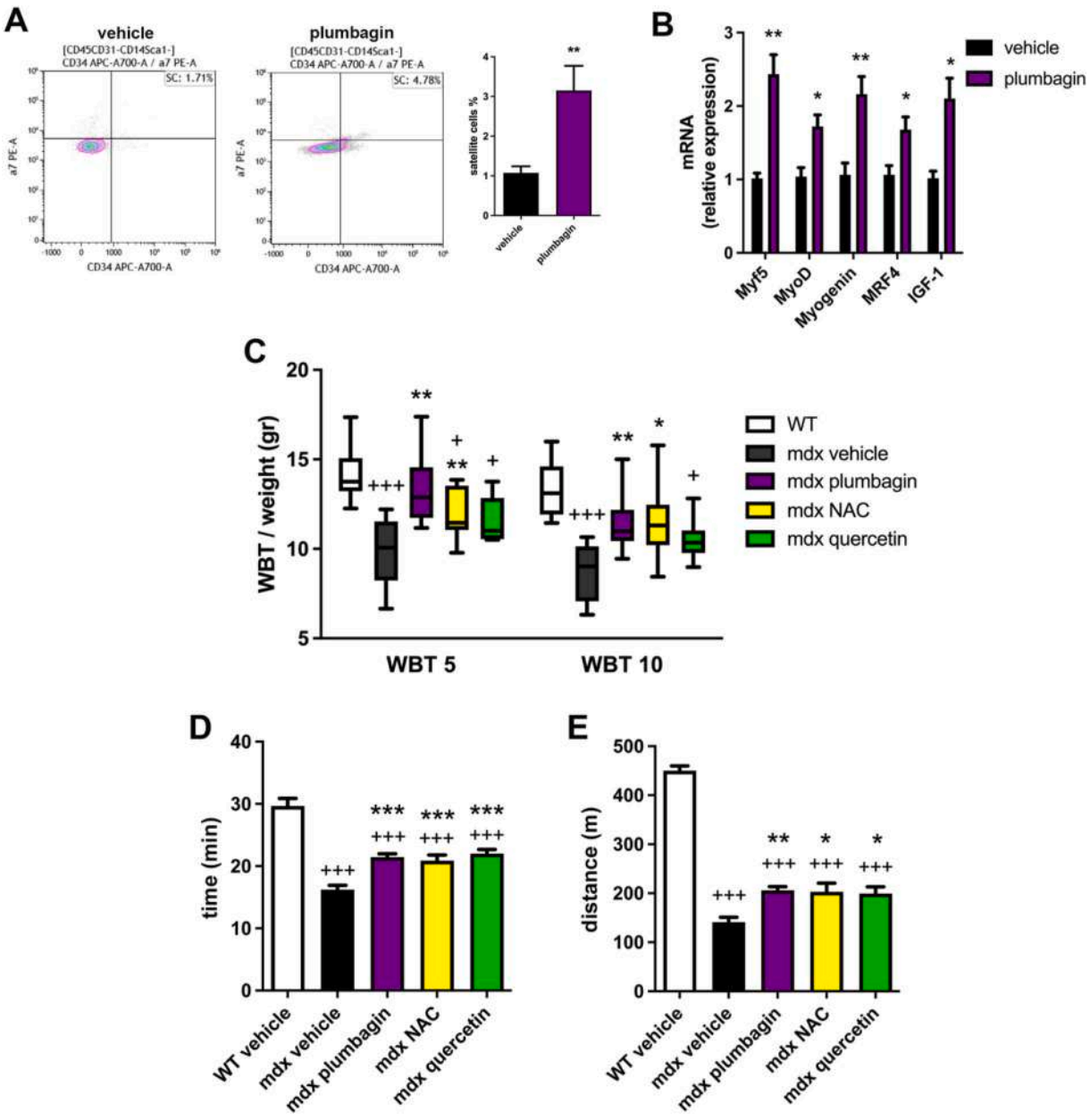

Fig. 4. ***Effect of plumbagin on muscle regeneration and function of mdx mice.*** (A) Representative density plots (panel on the left) and satellite cell quantification (graph on the right) by flow cytometry in hindlimb muscles of mdx mice treated with vehicle or plumbagin. Values are expressed as mean ± SEM (n = 9 mice per group) normalized vs. the vehicle treated mice. **p < 0.01 vs. the vehicle. (B) RT-qPCR analysis of myogenic markers Myf5, MyoD, Myogenin, MRF4 and IGF-1 of tibialis anterior of mdx mice treated with vehicle or plumbagin. Values are expressed as mean ± SEM (n ≥ 5 mice) normalized vs. the vehicle treated mice. *p < 0.05, **p < 0.01 vs. the vehicle. (C) WBT measurements determined by dividing the average of the top five or top ten forward pulling tensions by the body weight in wt treated vehicle and mdx mice treated with vehicle, plumbagin, NAC and quercetin after 3 months of treatment. Values are expressed as mean ± SEM. + p < 0.05, +++ p < 0.001 vs. the wt vehicle group; *p < 0.05, **p < 0.01 vs. the mdx vehicle group (n ≥ 9 mice per group). (D–E) Evaluation of muscle performance by exhaustion treadmill running test, measuring the running time (D) and the distance to exhaustion (E) in wt and mdx mice. Values are expressed as mean ± SEM. +++ p < 0.001 vs. the wt vehicle group; *p < 0.05, **p < 0.01, ***p < 0.001 vs. the mdx vehicle group (n ≥ 7 mice per group).

functional full-length dystrophin [46,64]. Noteworthy, the fruit fly is emerging as a very potent *in vivo* tool for studying the human disease in combination with the more traditional vertebrate systems, as well as its potential for drug discovery, including bioactive natural compounds [65–70]. In this regard, the oral bioavailability and the protective role of plumbagin in Drosophila models of metabolic dysfunctions and infections have been recently reported [20,71].

As this was the first study using plumbagin in DMD *in vivo*, we tested the maximum tolerated dose in flies by diet supplement with increasing amounts of plumbagin; according to previous reports in other models [20,71], we identified 1 nM and 30 nM as non-toxic concentrations to be administered orally in both wt and Dys^{E17} strain. In mdx mice we tested a concentration of 250 mg/kg/day in the food that allowed a dosage of *c. a.* 30 mg/kg/day as a comparable dosage regimen has already demonstrated to be effective in rodent models of inflammation and diabetes without any signs of toxicity [47,48]. Since several studies have shown a positive effect of antioxidant treatment in young mdx mice [54,72–75] we began to administer plumbagin to 1 month-old animals. We detected plumbagin in the blood thus demonstrating its systemic delivery upon ingestion. Also, no signs of distress or pathology attributable to drug adverse reactions were observed during the period of treatment. We found that the growth of the animals was similar to that of control

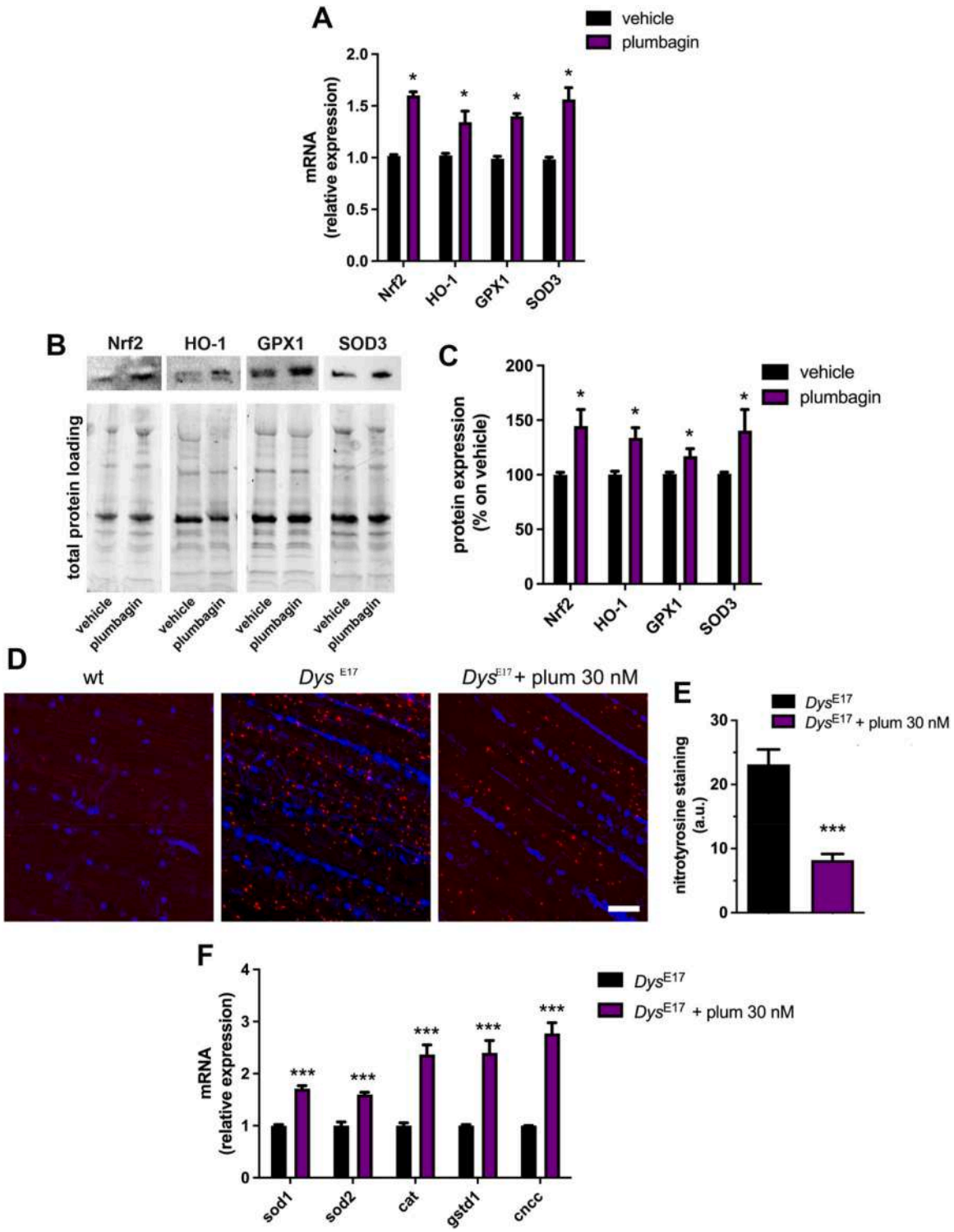

Fig. 5. ***The antioxidant effect of plumbagin in dystrophic mice and*** **D*rosophila.*** (A–C) Oxidative stress in mdx mice treated with plumbagin for 3 months. (A) RT-qPCR analysis of the antioxidant defense system gene, Nrf2, HO-1, GPX1 and SOD3, in mdx mice treated with vehicle or plumbagin. Values are expressed as mean ± SEM ($n \geq 5$ mice per group) normalized vs. the vehicle treated mice. *$p < 0.05$ vs. the vehicle. (B–C) Western blotting analysis of the antioxidant defense system gene, Nrf2, HO-1, GPX1 and SOD3, in mdx mice treated with vehicle or plumbagin. (B) Representative images of the protein expression normalized on total protein content. (C) Quantification of the protein expression assessed by densitometry. Values are expressed as mean ± SEM ($n \geq 4$ mice per group) *$p < 0.05$, vs. the vehicle. (D–F) Oxidative stress in muscles of eclosed fly adults raised for 20 days in the absence and in the presence of 30 nM plumbagin in the food. (D) Confocal microscopy immunofluorescence imaging of nitrotyrosine (red dots) in DLM longitudinal sections of wt, Dys^{E17}, and Dys^{E17} + plumbagin. Nuclei were stained with DAPI (blue). Scale bar= 20 μm. (E) The graph depicts the quantitative analysis of DLM nitrotyrosine staining (fluorescence level). Results are expressed as arbitrary units (a.u.). ***$p < 0.0001$ vs. Dys^{E17}. Images and data are representative of 8 animals obtained from 3 independent experiments. (F) RT-qPCR of oxidative-related genes in DLM of Dys^{E17} and Dys^{E17} + plumbagin. Results are expressed as fold change of Dys^{E17}. ***$p < 0.0001$ vs. Dys^{E17}. Data are representative of 45 animals obtained from 3 independent experiments.

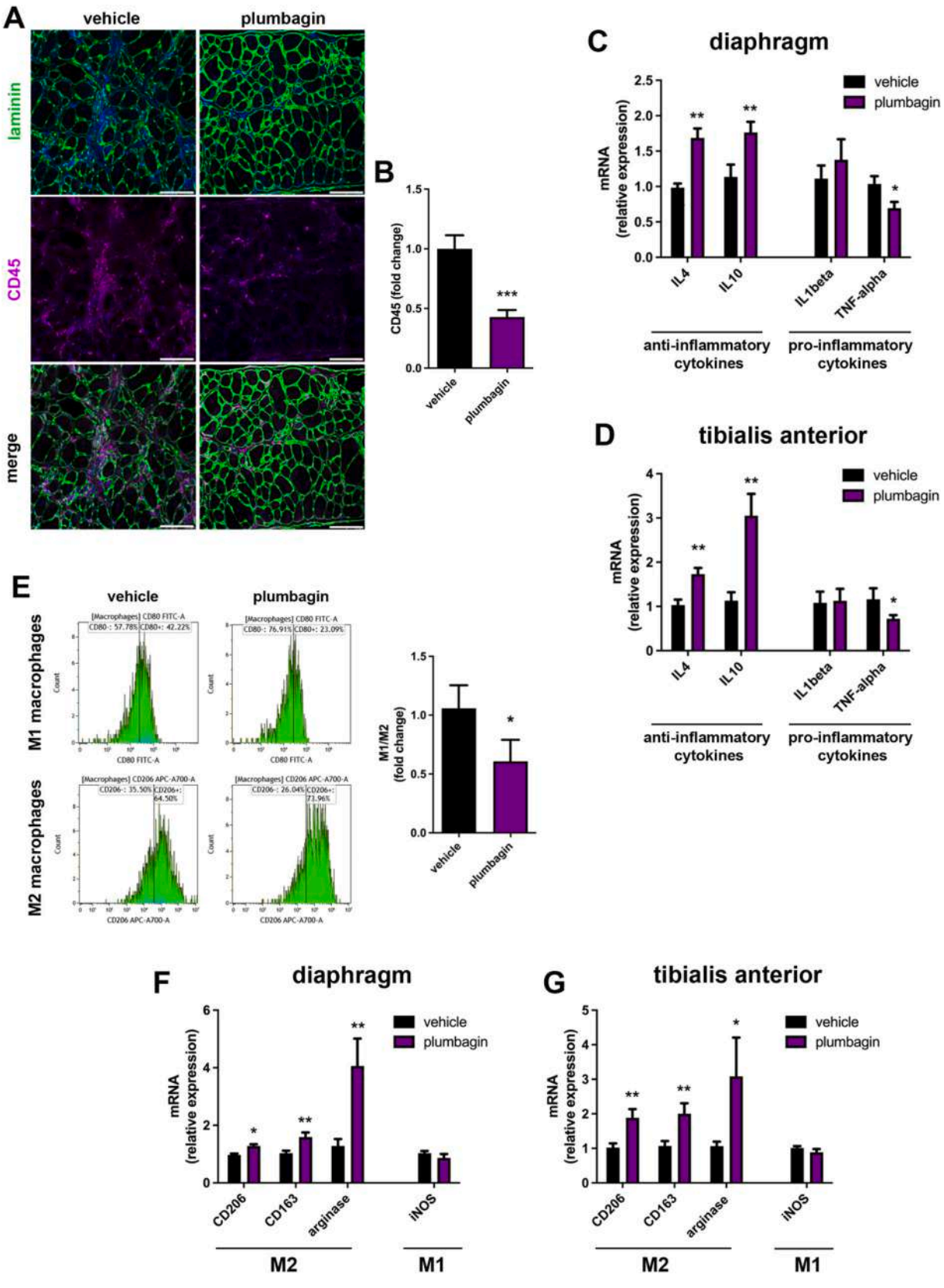

(caption on next page)

Fig. 6. ***The anti-inflammatory effect of plumbagin in dystrophic mice.*** (A) Representative images of CD45 immunostaining (purple) of sections of diaphragms of mdx mice treated with vehicle or plumbagin for 3 months. Laminin (green) was used as sarcolemma marker to identify fiber; nuclei were stained with DAPI (blue) (scale bar = 100 μm). (B) The graph shows CD45 quantification. Values are expressed as fold change compared to the vehicle (mean ± SEM; n = 3 mice per group). ***p < 0.001 vs. vehicle. (C–D) RT-qPCR analysis of the anti-inflammatory cytokines IL4 and IL10 and the pro-inflammatory cytokines IL1beta and TNF-alpha of diaphragm (C) and tibialis anterior (D) muscles of mdx mice treated with vehicle or plumbagin. Values are expressed as mean ± SEM (n ≥ 5 mice per group) normalized vs. the vehicle treated mice. *p < 0.05, **p < 0.01 vs. the vehicle. (E) M1/M2 macrophage ratio in hindlimb muscles of mdx mice treated with vehicle or plumbagin. The images show representative histograms of cell surface analysis expression by flow cytometry of CD80 (M1 marker) and CD206 (M2 marker). The graph on the left shows the quantification of the M1/M2 ratio. Values are expressed as fold change compared to the vehicle (mean ± SEM; n ≥ 9 mice per group). *p < 0.05 vs. vehicle. (F–G) RT-qPCR analysis of the M2 markers CD206, CD163 and arginase and the M1 marker iNOS of diaphragm (F) and tibialis anterior (G) muscles of mdx mice treated with vehicle or plumbagin. Values are expressed as mean ± SEM (n ≥ 5 mice per group) normalized vs. the vehicle treated mice. *p < 0.05, **p < 0.01 vs. the vehicle.

(untreated) mice indicating that the compound was safe throughout the experimental setting. These observations are relevant to overcome two main issues concerning the translational use of plumbagin in *in vivo* systems: the poor bioavailability after oral administration and the potential toxicity due to its pro-oxidant effect when reaching high concentrations at cellular level [22,76,77].

Nrf2 is a transcription factor that upregulates the expression of many cytoprotective genes, containing the so-called sequence ARE (Antioxidant Response Elements), in response to oxidants and other stress factors. Over 250 genes are regulated by Nrf2/ARE and encode for enzymes involved in antioxidant defense and detoxification. These genes include: i) the classic phase II detoxification enzymes; ii) the enzymes involved in the biosynthesis of GSH and its antioxidant system, e.g. GPx family, among which GPx1 is the most abundant isoenzyme and it is ubiquitous in cytoplasm and mitochondria [78]; iii) the HO-1, which besides removing toxic heme, produces biliverdin, a potent antioxidant [79]; and iv) the SODs, enzymes responsible for the dismutation (simultaneous oxidation and reduction) and breakdown of superoxide radicals into molecular oxygen and hydrogen peroxide [80]. Because of this pleiotropic action, Nrf2 influences key molecular responses and has the potential to simultaneously modulate several pathological features of DMD thus widening the therapeutic benefits of its modulation [81]. In this study we demonstrate that plumbagin exerted a robust antioxidant effect in dystrophic skeletal muscle by acting on Nrf2 antioxidant defense system. Specifically, non-toxic plumbagin dose inhibited muscle peroxynitrite generation in *Dys*^{E17} flies, thus positively affecting their redox steady state. Accordingly, SOD and CAT, two universal detoxifying enzymes of aerobic organisms, were upregulated as well as the levels of GstD1, a prototypical oxidative stress response enzyme in flies and a prominent target of Nrf2 [61,82,83]. Consistently plumbagin increases the transcription of Nrf2 (CncC) itself thus sustaining the induction of signaling enzymes counteracting ROS unbalance. This likely account for the protective mechanism of plumbagin-induced antioxidant activity in DMD muscles. Similar actions have been recently described in Drosophila nervous system after plumbagin treatment [20].

In mdx mice treated with plumbagin besides the increase of Nrf2, we also observed a higher expression of HO-1, GPX1 and SOD3 compared to control mice. An altered expression of HO-1 in DMD has been already reported [84]. In mdx mice, the expression of HO-1 in limb muscles and diaphragm has been found higher than in wt animals, remaining consistently elevated from 8 up to 52 weeks. In addition, pharmacological inhibition of HO-1 activity or genetic silencing has been shown to exacerbate muscle damage and inflammation in the murine model [84]. An impairment of HO-1 has also been observed in young children affected by DMD. This seems to be associated with a consistent up-regulation of the cytokine IL6 and might predispose to a redundant inflammatory response during the progression of the disease or to a delay in the resolution of early inflammation [85]. Reports in the literature shows an increase of GPx1 as well as other enzymes of the antioxidant defense system in the muscles of mdx mice as a compensatory mechanism of ROS production in the pathology [28–30]. However, there is currently a lack of knowledge about the pharmacological and cellular modulation of these antioxidant enzymes in DMD. All of them have been found upregulated in tibialis anterior muscle of an acute damage mouse model, in which inflammation was modulated by the Nrf2 pathway [37], analogously to GPx1 and SOD3 in human skeletal muscle subjected to damage induced by intense exercise after polyphenol supplementation [86]. Notably, the positive modulation of the antioxidant defense system paralleled with an improvement in muscle recovery after injury. Our findings on the impact of plumbagin on Nrf2 pathway are in line with these results and account for the positive action of the compound in dystrophic muscle structure and function. They also strongly suggest the antioxidant activity as the mechanism behind the protective effect of plumbagin against DMD.

Dystrophic flies are a good model for age-dependent onset of DMD showing decreased lifespan, progressive impairment of climbing ability and muscle degeneration [31,32,34]. To note, *Dys*^{E17} flies orally administered with non-toxic plumbagin displayed dose-dependent increase of survival rate. Climbing defects and damaged muscle also markedly recovered, thus indicating the positive effects of plumbagin on DMD phenotype both ameliorating the animal health/lifespan and the muscle structure/function. In this line, in mdx mice plumbagin ameliorated muscle phenotype and counteracted inflammation in the diaphragm and tibialis anterior, by increasing the expression of anti-inflammatory cytokines and promoting the shift of macrophages inside the skeletal muscles toward an anti-inflammatory M2 phenotype. The crosstalk between the induction of M2 polarization and antioxidant activity has been already described for compounds such as curcumin, NAC, quercetin, resveratrol, and sulforaphane [87–92]. Moreover, the anti-inflammatory effect of plumbagin has been observed in different pathological conditions [93–95]. For instance, plumbagin restored the vasodilatory responses in human skeletal muscle feed arteries in vitro [96], as well as protected rat heart tissues from cardiotoxic damage, also inhibiting inflammation and increasing the antioxidant status [97]. Of note, in an experimental model of hepatic injury the reduction of inflammation was found to be related to the increase of GPx activity [93].

As mentioned above, the negative modulation of inflammation by plumbagin was associated with the amelioration of muscle morphology, the reduction of myonecrosis and collagen deposition (fibrosis) as well as the increase of regeneration (terminal regenerated fibers), resulting in the significant improvement of skeletal muscle force in sedentary animals. The positive effect of plumbagin led to a better muscle performance of mdx mice also in the final endurance test. Notably, two antioxidant compounds, NAC and quercetin, already proved as effective in the mdx model [52–56] were somewhat active in our system although less than plumbagin.

This study has certain limitations mostly concerning the use of the mdx model and the length of the treatment. Indeed, despite lacking dystrophin, like patients affected by DMD, mdx mice have a milder phenotype, and more severe clinical and pathological features can be observed in elderly mice [98]. Therefore, further experiments analyzing the chronic effect of plumbagin in older mice may help to assess the translatability of our results in longer duration studies.

In conclusion, DMD is a complex disease with multifactorial pathological mechanism of muscle regeneration and degeneration namely involving mechanisms as crucial as mitochondrial dysfunction, oxidative stress and inflammation, all containing several possible therapeutic

targets. Our evidence corroborates the targeting of oxidative stress as valuable, evolutionary conserved, therapeutic option in DMD and suggests the pharmacological and nutraceutical potential of plumbagin for muscle health.

Funding

This work was supported by the Association Française contre les Myopathies AFM-Telethon (Grant number 23172) to C. Perrotta and S. Hrelia, Ministero dell'Università e Ricerca, "PRIN2020" (2020ELYA32 004) to E. Clementi and D. Cervia and "PRIN2022" (G53D2300517 0006) to C. Perrotta.

CRediT authorship contribution statement

Davide Cervia: Writing – review & editing, Writing – original draft, Conceptualization, Formal analysis, Supervision, Funding acquisition. **Silvia Zecchini:** Investigation, Formal analysis, Visualization. **Luca Pincigher:** Investigation, Formal analysis. **Paulina Roux-Biejat:** Investigation, Formal analysis. **Chiara Zalambani:** Investigation. **Elisabetta Catalani:** Investigation, Visualization. **Alessandro Arcari:** Investigation. **Simona Del Quondam:** Investigation. **Kashi Brunetti:** Investigation. **Roberta Ottria:** Methodology. **Sara Casati:** Investigation. **Claudia Vanetti:** Investigation. **Maria Cristina Barbalace:** Formal analysis. **Cecilia Prata:** Methodology, Formal analysis. **Marco Malaguti:** Methodology. **Silvia Rosanna Casati:** Investigation. **Laura Lociuro:** Investigation. **Matteo Giovarelli:** Investigation. **Emanuele Mocciaro:** Writing – original draft, Validation. **Sestina Falcone:** Methodology. **Claudio Fenizia:** Methodology. **Claudia Moscheni:** Methodology. **Silvana Hrelia:** Writing – original draft, Funding acquisition, Resources. **Clara De Palma:** Writing – original draft, Validation. **Emilio Clementi:** Writing – original draft, Resources, Funding acquisition. **Cristiana Perrotta:** Writing – review & editing, Writing – original draft, Conceptualization, Visualization, Formal analysis, Validation, Resources, Supervision, Funding acquisition, Project administration.

Declaration of competing interest

The authors declare that they have no known competing financial interests or personal relationships that could have appeared to influence the work reported in this paper.

Acknowledgments

The Ph.D. student Luca Pincigher was financed by the European Union - NexrGenerationEU through the Italian Ministry of University and Resaerch under PNRR – Mission 4 Component 2, Investement 3.3 (DM 117/2023). The Ph.D. Student Chiara Zalambani was financed by the European Union - NexrGenerationEU through the Italian Ministry of University and Resaerch under PNRR – Mission 4 Component 1, Investement 4.1 (DM 118/2023). The PhD Silvia Rosanna Casati and Laura Lociuro were supported by the Ph.D. program in Experimental Medicine of the Università degli Studi di Milano.

Appendix A. Supplementary data

Supplementary data to this article can be found online at https://doi.org/10.1016/j.freeradbiomed.2024.09.037.

References

[1] E. Mercuri, C.G. Bönnemann, F. Muntoni, Muscular dystrophies, Lancet 394 (2019) 2025–2038, https://doi.org/10.1016/S0140-6736(19)32910-1.
[2] D. Duan, N. Goemans, S. Takeda, E. Mercuri, A. Aartsma-Rus, Duchenne muscular dystrophy, Nat Rev Dis Primers 7 (2021) 13, https://doi.org/10.1038/s41572-021-00248-3.
[3] Q.Q. Gao, E.M. McNally, The dystrophin complex: structure, function, and implications for therapy, Compr. Physiol. 5 (2015) 1223–1239, https://doi.org/10.1002/cphy.c140048.
[4] M. Chang, Y. Cai, Z. Gao, X. Chen, B. Liu, C. Zhang, W. Yu, Q. Cao, Y. Shen, X. Yao, X. Chen, H. Sun, Duchenne muscular dystrophy: pathogenesis and promising therapies, J. Neurol. 270 (2023) 3733–3749, https://doi.org/10.1007/s00415-023-11796-x.
[5] M.R.F. Gosselin, V. Mournetas, M. Borczyk, S. Verma, A. Occhipinti, J. Róg, L. Bozycki, M. Korostynski, S.C. Robson, C. Angione, C. Pinset, D.C. Gorecki, Loss of full-length dystrophin expression results in major cell-autonomous abnormalities in proliferating myoblasts, Elife 11 (2022), https://doi.org/10.7554/eLife.75521.
[6] T.C. Roberts, M.J.A. Wood, K.E. Davies, Therapeutic approaches for Duchenne muscular dystrophy, Nat. Rev. Drug Discov. 22 (2023) 917–934, https://doi.org/10.1038/s41573-023-00775-6.
[7] V. Ricotti, D.A. Ridout, E. Scott, R. Quinlivan, S.A. Robb, A.Y. Manzur, F. Muntoni, A. Manzur, F. Muntoni, S. Robb, R. Quinlivan, V. Ricotti, M. Main, K. Bushby, V. Straub, A. Sarkozy, M. Guglieri, E. Strehle, M. Eagle, A. Mayhew, H. Roper, H. McMurchie, A. Childs, K. Pysden, L. Pallant, S. Spinty, G. Peachey, A. Shillington, E. Wraige, H. Jungbluth, J. Sheehan, R. Spahr, I. Hughes, E. Bateman, C. Cammiss, T. Willis, L. Groves, N. Emery, P. Baxter, M. Senior, L. Hartley, B. Parsons, A. Majumdar, L. Jenkins, K. Naismith, A. Keddie, I. Horrocks, M. Di Marco, G. Chow, A. Miah, C. de Goede, N. Thomas, M. Geary, J. Palmer, C. White, K. Greenfield, E. Scott, Long-term benefits and adverse effects of intermittent versus daily glucocorticoids in boys with Duchenne muscular dystrophy, J. Neurol. Neurosurg. Psychiatry 84 (2013) 698–705, https://doi.org/10.1136/jnnp-2012-303902.
[8] C.M. McDonald, E.K. Henricson, R.T. Abresch, T. Duong, N.C. Joyce, F. Hu, P. R. Clemens, E.P. Hoffman, A. Cnaan, H. Gordish-Dressman, C.I.N.R. G. Investigators, Long-term effects of glucocorticoids on function, quality of life, and survival in patients with Duchenne muscular dystrophy: a prospective cohort study, Lancet 391 (2018) 451–461, https://doi.org/10.1016/S0140-6736(17)32160-8.
[9] H. Zhang, G. Qi, K. Wang, J. Yang, Y. Shen, X. Yang, X. Chen, X. Yao, X. Gu, L. Qi, C. Zhou, H. Sun, Oxidative stress: roles in skeletal muscle atrophy, Biochem. Pharmacol. 214 (2023) 115664, https://doi.org/10.1016/j.bcp.2023.115664.
[10] K. Woodman, C. Coles, S. Lamandé, J. White, Nutraceuticals and their potential to treat duchenne muscular dystrophy: separating the credible from the conjecture, Nutrients 8 (2016) 713, https://doi.org/10.3390/nu8110713.
[11] B. Boccanegra, I.E.C. Verhaart, O. Cappellari, E. Vroom, A. De Luca, Safety issues and harmful pharmacological interactions of nutritional supplements in Duchenne muscular dystrophy: considerations for Standard of Care and emerging virus outbreaks, Pharmacol. Res. 158 (2020) 104917, https://doi.org/10.1016/j.phrs.2020.104917.
[12] I. Suntar, A. Sureda, T. Belwal, A. Sanches Silva, R.A. Vacca, D. Tewari, E. Sobarzo-Sánchez, S.F. Nabavi, S. Shirooie, A.R. Dehpour, S. Xu, B. Yousefi, M. Majidinia, M. Daglia, G. D'Antona, S.M. Nabavi, Natural products, PGC-1 , and Duchenne muscular dystrophy, Acta Pharm. Sin. B 10 (2020) 734–745, https://doi.org/10.1016/j.apsb.2020.01.001.
[13] S.R. Casati, D. Cervia, P. Roux-Biejat, C. Moscheni, C. Perrotta, C. De Palma, Mitochondria and reactive oxygen species: the therapeutic balance of powers for duchenne muscular dystrophy, Cells 13 (2024) 574, https://doi.org/10.3390/cells13070574.
[14] N. Kapoor, P. Kandwal, G. Sharma, L. Gambhir, Redox ticklers and beyond: naphthoquinone repository in the spotlight against inflammation and associated maladies, Pharmacol. Res. 174 (2021) 105968, https://doi.org/10.1016/j.phrs.2021.105968.
[15] A. Roy, N. Bharadvaja, Biotechnological approaches for the production of pharmaceutically important compound: plumbagin, Curr Pharm Biotechnol 19 (2018) 372–381, https://doi.org/10.2174/1389201019666180629143842.
[16] S. Padhye, P. Dandawate, M. Yusufi, A. Ahmad, F.H. Sarkar, Perspectives on medicinal properties of plumbagin and its analogs, Med. Res. Rev. 32 (2012) 1131–1158, https://doi.org/10.1002/med.20235.
[17] P. Panichayupakaranant, M.I. Ahmad, Plumbagin and its role in chronic diseases, Adv. Exp. Med. Biol. 929 (2016) 229–246, https://doi.org/10.1007/978-3-319-41342-6_10.
[18] S. Rajalakshmi, N. Vyawahare, A. Pawar, P. Mahaparale, B. Chellampillai, Current development in novel drug delivery systems of bioactive molecule plumbagin, Artif. Cells, Nanomed. Biotechnol. 46 (2018) 209–218, https://doi.org/10.1080/21691401.2017.1417865.
[19] A. Roy, Plumbagin: a potential anti-cancer compound, Mini Rev. Med. Chem. 21 (2021) 731–737, https://doi.org/10.2174/1389557520666201116144421.
[20] E. Catalani, S. Del Quondam, K. Brunetti, A. Cherubini, S. Bongiorni, A.R. Taddei, S. Zecchini, M. Giovarelli, C. De Palma, C. Perrotta, E. Clementi, G. Prantera, D. Cervia, Neuroprotective role of plumbagin on eye damage induced by high-sucrose diet in adult fruit fly Drosophila melanogaster, Biomed. Pharmacother. 166 (2023) 115298, https://doi.org/10.1016/j.biopha.2023.115298.
[21] T.B. Santos, L.G.C. de Moraes, P.A.F. Pacheco, D.G. Dos Santos, R.M. de, A. C. Ribeiro, C.D.S. Moreira, D.R. da Rocha, Naphthoquinones as a promising class of compounds for facing the challenge of Parkinson's disease, Pharmaceuticals 16 (2023), https://doi.org/10.3390/ph16111577.
[22] G. Petrocelli, P. Marrazzo, L. Bonsi, F. Facchin, F. Alviano, S. Canaider, Plumbagin, a natural compound with several biological effects and anti-inflammatory properties, Life 13 (2023) 1303, https://doi.org/10.3390/life13061303.
[23] M.K. Pandey, S.C. Gupta, D. Karelia, P.J. Gilhooley, M. Shakibaei, B.B. Aggarwal, Dietary nutraceuticals as backbone for bone health, Biotechnol. Adv. 36 (2018) 1633–1648, https://doi.org/10.1016/j.biotechadv.2018.03.014.

[24] S.K. Tripathi, M. Panda, B.K. Biswal, Emerging role of plumbagin: cytotoxic potential and pharmaceutical relevance towards cancer therapy, Food Chem. Toxicol. 125 (2019) 566–582, https://doi.org/10.1016/j.fct.2019.01.018.
[25] S. Zhang, D. Li, J.-Y. Yang, T.-B. Yan, Plumbagin protects against glucocorticoid-induced osteoporosis through Nrf-2 pathway, Cell Stress Chaperones 20 (2015) 621–629, https://doi.org/10.1007/s12192-015-0585-0.
[26] W. Zhang, L. Cheng, Y. Hou, M. Si, Y.-P. Zhao, L. Nie, Plumbagin protects against spinal cord injury-induced oxidative stress and inflammation in wistar rats through nrf-2 upregulation, Drug Res. 65 (2014) 495–499, https://doi.org/10.1055/s-0034-1389950.
[27] W. Kuan-hong, L. Bai-zhou, Plumbagin protects against hydrogen peroxide-induced neurotoxicity by modulating NF-κB and Nrf-2, Arch. Med. Sci. 14 (2018) 1112–1118, https://doi.org/10.5114/aoms.2016.64768.
[28] J.J. Kaczor, J.E. Hall, E. Payne, M.A. Tarnopolsky, Low intensity training decreases markers of oxidative stress in skeletal muscle of mdx mice, Free Radic. Biol. Med. 43 (2007) 145–154, https://doi.org/10.1016/j.freeradbiomed.2007.04.003.
[29] M.-H. Disatnik, J. Dhawan, Y. Yu, M.F. Beal, M.M. Whirl, A.A. Franco, T.A. Rando, Evidence of oxidative stress in mdx mouse muscle: studies of the pre-necrotic state, J. Neurol. Sci. 161 (1998) 77–84, https://doi.org/10.1016/S0022-510X(98)00258-5.
[30] R.J. Ragusa, C.K. Chow, J.D. Porter, Oxidative stress as a potential pathogenic mechanism in an animal model of Duchenne muscular dystrophy, Neuromuscul. Disord. 7 (1997) 379–386, https://doi.org/10.1016/S0960-8966(97)00096-5.
[31] R.E. Kreipke, Y.V. Kwon, H.R. Shcherbata, H. Ruohola-Baker, in: Drosophila melanogaster as a Model of Muscle Degeneration Disorders, 2017, https://doi.org/10.1016/bs.ctdb.2016.07.003, 83–109.
[32] S. Potikanond, W. Nimlamool, J. Noordermeer, L.G. Fradkin, in: Muscular Dystrophy Model, 2018, https://doi.org/10.1007/978-981-13-0529-0_9, 147–172.
[33] E. Catalani, F. Silvestri, S. Bongiorni, A.R. Taddei, G. Fanelli, S. Rinalducci, C. De Palma, C. Perrotta, G. Prantera, D. Cervia, Retinal damage in a new model of hyperglycemia induced by high-sucrose diets, Pharmacol. Res. 166 (2021) 105488, https://doi.org/10.1016/j.phrs.2021.105488.
[34] H.R. Shcherbata, A.S. Yatsenko, L. Patterson, V.D. Sood, U. Nudel, D. Yaffe, D. Baker, H. Ruohola-Baker, Dissecting muscle and neuronal disorders in a Drosophila model of muscular dystrophy, EMBO J. 26 (2007) 481–493, https://doi.org/10.1038/sj.emboj.7601503.
[35] S.A. Deshpande, R. Yamada, C.M. Mak, B. Hunter, A. Soto Obando, S. Hoxha, W. W. Ja, Acidic food pH increases palatability and consumption and extends Drosophila lifespan, J. Nutr. 145 (2015) 2789–2796, https://doi.org/10.3945/jn.115.222380.
[36] C. De Palma, F. Morisi, S. Pambianco, E. Assi, T. Touvier, S. Russo, C. Perrotta, V. Romanello, S. Carnio, V. Cappello, P. Pellegrino, C. Moscheni, M.T. Bassi, M. Sandri, D. Cervia, E. Clementi, Deficient nitric oxide signalling impairs skeletal muscle growth and performance: involvement of mitochondrial dysregulation, Skelet Muscle 4 (2014) 22, https://doi.org/10.1186/s13395-014-0022-6.
[37] P. Roux-Biejat, M. Coazzoli, P. Marrazzo, S. Zecchini, I. Di Renzo, C. Prata, A. Napoli, C. Moscheni, M. Giovarelli, M.C. Barbalace, E. Catalani, M.T. Bassi, C. De Palma, D. Cervia, M. Malaguti, S. Hrelia, E. Clementi, C. Perrotta, Acid sphingomyelinase controls early phases of skeletal muscle regeneration by shaping the macrophage phenotype, Cells 10 (2021) 3028, https://doi.org/10.3390/cells10113028.
[38] C. Perrotta, F. Buonanno, S. Zecchini, A. Giavazzi, F. Proietti Serafini, E. Catalani, L. Guerra, M.C. Belardinelli, S. Picchietti, A.M. Fausto, S. Giorgi, E. Marcantoni, E. Clementi, C. Ortenzi, D. Cervia, Climacostol reduces tumour progression in a mouse model of melanoma via the p53-dependent intrinsic apoptotic programme, Sci. Rep. 6 (2016) 27281, https://doi.org/10.1038/srep27281.
[39] M. Uboldi, C. Perrotta, C. Moscheni, S. Zecchini, A. Napoli, C. Castiglioni, A. Gazzaniga, A. Melocchi, L. Zema, Insights into the safety and versatility of 4D printed intravesical drug delivery systems, Pharmaceutics 15 (2023) 757, https://doi.org/10.3390/pharmaceutics15030757.
[40] M. Coazzoli, A. Napoli, P. Roux-Biejat, C. De Palma, C. Moscheni, E. Catalani, S. Zecchini, V. Conte, M. Giovarelli, S. Caccia, P. Procacci, D. Cervia, E. Clementi, C. Perrotta, Acid sphingomyelinase downregulation enhances mitochondrial fusion and promotes oxidative metabolism in a mouse model of melanoma, Cells 9 (2020) 848, https://doi.org/10.3390/cells9040848.
[41] E. Mocciaro, R. Giambruno, S. Micheloni, F.M. Cernilogar, A. Andolfo, C. Consonni, M. Pannese, G. Ferri, V. Runfola, G. Schotta, D. Gabellini, WDR5 is required for *DUX4* expression and its pathological effects in FSHD muscular dystrophy, Nucleic Acids Res. 51 (2023) 5144–5161, https://doi.org/10.1093/nar/gkad230.
[42] R.O. Esenaliev, I.Y. Petrov, Y. Petrov, J. Guptarak, D.R. Boone, E. Mocciaro, H. Weisz, M.A. Parsley, S.L. Sell, H. Hellmich, J.M. Ford, C. Pogue, D. DeWitt, D. S. Prough, M.-A. Micci, Nano-pulsed laser therapy is neuroprotective in a rat model of blast-induced neurotrauma, J. Neurotrauma 35 (2018) 1510–1522, https://doi.org/10.1089/neu.2017.5249.
[43] M. Giovarelli, S. Zecchini, E. Martini, M. Garrè, S. Barozzi, M. Ripolone, L. Napoli, M. Coazzoli, C. Vantaggiato, P. Roux-Biejat, D. Cervia, C. Moscheni, C. Perrotta, D. Parazzoli, E. Clementi, C. De Palma, Drp1 overexpression induces desmin disassembling and drives kinesin-1 activation promoting mitochondrial trafficking in skeletal muscle, Cell Death Differ. 27 (2020) 2383–2401, https://doi.org/10.1038/s41418-020-0510-7.
[44] M.C. Barbalace, M. Freschi, I. Rinaldi, E. Mazzara, T. Maraldi, M. Malaguti, C. Prata, F. Maggi, R. Petrelli, S. Hrelia, C. Angeloni, Identification of anti-neuroinflammatory bioactive compounds in essential oils and aqueous distillation residues obtained from commercial Varieties of cannabis sativa L, Int. J. Mol. Sci. 24 (2023) 16601, https://doi.org/10.3390/ijms242316601.
[45] S. Neuman, M. Kovalio, D. Yaffe, U. Nudel, The *Drosophila* homologue of the dystrophin gene – introns containing promoters are the major contributors to the large size of the gene, FEBS Lett. 579 (2005) 5365–5371, https://doi.org/10.1016/j.febslet.2005.08.073.
[46] E. Catalani, S. Bongiorni, A.R. Taddei, M. Mezzetti, F. Silvestri, M. Coazzoli, S. Zecchini, M. Giovarelli, C. Perrotta, C. De Palma, E. Clementi, M. Ceci, G. Prantera, D. Cervia, Defects of full-length dystrophin trigger retinal neuron damage and synapse alterations by disrupting functional autophagy, Cell. Mol. Life Sci. 78 (2021) 1615–1636, https://doi.org/10.1007/s00018-020-03598-5.
[47] C. Sunil, V. Duraipandiyan, P. Agastian, S. Ignacimuthu, Antidiabetic effect of plumbagin isolated from Plumbago zeylanica L. root and its effect on GLUT4 translocation in streptozotocin-induced diabetic rats, Food Chem. Toxicol. 50 (2012) 4356–4363, https://doi.org/10.1016/j.fct.2012.08.046.
[48] A.C. Gupta, S. Mohanty, A. Saxena, A.K. Maurya, D.U. Bawankule, Plumbagin, a vitamin K3 analogue ameliorate malaria pathogenesis by inhibiting oxidative stress and inflammation, Inflammopharmacology 26 (2018) 983–991, https://doi.org/10.1007/s10787-018-0465-1.
[49] N. Yanay, M. Rabie, Y. Nevo, Impaired regeneration in dystrophic muscle-new target for therapy, Front. Mol. Neurosci. 13 (2020) 69, https://doi.org/10.3389/fnmol.2020.00069.
[50] Y. Yoshimoto, M. Ikemoto-Uezumi, K. Hitachi, S. Fukada, A. Uezumi, Methods for accurate assessment of myofiber maturity during skeletal muscle regeneration, Front. Cell Dev. Biol. 8 (2020), https://doi.org/10.3389/fcell.2020.00267.
[51] T. Yoshida, P. Delafontaine, Mechanisms of IGF-1-mediated regulation of skeletal muscle hypertrophy and atrophy, Cells 9 (2020) 1970, https://doi.org/10.3390/cells9091970.
[52] H.R. Spaulding, C.G. Ballmann, J.C. Quindry, J.T. Selsby, Long-term quercetin dietary enrichment partially protects dystrophic skeletal muscle, PLoS One 11 (2016) e0168293, https://doi.org/10.1371/journal.pone.0168293.
[53] W. Lin, Y. Zhao, C. Liu, Y. Yan, Q. Ou, Quercetin supplementation and muscular atrophy in animal models: a systematic review and meta-analysis, Int. J. Food Prop. 25 (2022) 2166–2183, https://doi.org/10.1080/10942912.2022.2127764.
[54] R. de Senzi Moraes Pinto, R. Ferretti, L.H.R. Moraes, H.S. Neto, M.J. Marques, E. Minatel, N-Acetylcysteine treatment reduces TNF-α levels and myonecrosis in diaphragm muscle of mdx mice, Clinical Nutrition 32 (2013) 472–475, https://doi.org/10.1016/j.clnu.2012.06.001.
[55] J.R. Terrill, H.G. Radley-Crabb, M.D. Grounds, P.G. Arthur, N-Acetylcysteine treatment of dystrophic mdx mice results in protein thiol modifications and inhibition of exercise induced myofibre necrosis, Neuromuscul. Disord. 22 (2012) 427–434, https://doi.org/10.1016/j.nmd.2011.11.007.
[56] N.P. Whitehead, C. Pham, O.L. Gervasio, D.G. Allen, *N* -Acetylcysteine ameliorates skeletal muscle pathophysiology in *mdx* mice, J Physiol 586 (2008) 2003–2014, https://doi.org/10.1113/jphysiol.2007.148338.
[57] Q. Zhang, S. Zhao, W. Zheng, H. Fu, T. Wu, F. Hu, Plumbagin attenuated oxygen-glucose deprivation/reoxygenation-induced injury in human SH-SY5Y cells by inhibiting NOX4-derived ROS-activated NLRP3 inflammasome, Biosci. Biotechnol. Biochem. 84 (2020) 134–142, https://doi.org/10.1080/09168451.2019.1664893.
[58] M. Guida, T. Maraldi, E. Resca, F. Beretti, M. Zavatti, L. Bertoni, G.B. La Sala, A. De Pol, Inhibition of nuclear Nox4 activity by plumbagin: effect on proliferative capacity in human amniotic stem cells, Oxid. Med. Cell. Longev. 2013 (2013) 1–12, https://doi.org/10.1155/2013/680816.
[59] Y. Ding, Z.-J. Chen, S. Liu, D. Che, M. Vetter, C.-H. Chang, Inhibition of Nox-4 activity by plumbagin, a plant-derived bioactive naphthoquinone, J. Pharm. Pharmacol. 57 (2010) 111–116, https://doi.org/10.1211/0022357055119.
[60] N.P. Whitehead, E.W. Yeung, S.C. Froehner, D.G. Allen, Skeletal muscle NADPH oxidase is increased and triggers stretch-induced damage in the mdx mouse, PLoS One 5 (2010) e15354, https://doi.org/10.1371/journal.pone.0015354.
[61] A. Pitoniak, D. Bohmann, Mechanisms and functions of Nrf2 signaling in Drosophila, Free Radic. Biol. Med. 88 (2015) 302–313, https://doi.org/10.1016/j.freeradbiomed.2015.06.020.
[62] A.S. Rosenberg, M. Puig, K. Nagaraju, E.P. Hoffman, S.A. Villalta, V.A. Rao, L. M. Wakefield, J. Woodcock, Immune-mediated pathology in Duchenne muscular dystrophy, Sci. Transl. Med. 7 (2015) 299rv4, https://doi.org/10.1126/scitranslmed.aaa7322.
[63] S.A. Villalta, B. Deng, C. Rinaldi, M. Wehling-Henricks, J.G. Tidball, IFN-γ promotes muscle damage in the mdx mouse model of Duchenne muscular dystrophy by suppressing M2 macrophage activation and inhibiting muscle cell proliferation, J. Immunol. 187 (2011) 5419–5428, https://doi.org/10.4049/jimmunol.1101267.
[64] E. Catalani, S. Zecchini, M. Giovarelli, A. Cherubini, S. Del Quondam, K. Brunetti, F. Silvestri, P. Roux-Biejat, A. Napoli, S.R. Casati, M. Ceci, N. Romano, S. Bongiorni, G. Prantera, E. Clementi, C. Perrotta, C. De Palma, D. Cervia, RACK1 is evolutionary conserved in satellite stem cell activation and adult skeletal muscle regeneration, Cell Death Discov 8 (2022) 459, https://doi.org/10.1038/s41420-022-01250-8.
[65] U.B. Pandey, C.D. Nichols, Human disease models in *Drosophila melanogaster* and the role of the fly in therapeutic drug discovery, Pharmacol. Rev. 63 (2011) 411–436, https://doi.org/10.1124/pr.110.003293.
[66] M. Xiu, Y. Wang, D. Yang, X. Zhang, Y. Dai, Y. Liu, X. Lin, B. Li, J. He, Using Drosophila melanogaster as a suitable platform for drug discovery from natural products in inflammatory bowel disease, Front. Pharmacol. 13 (2022), https://doi.org/10.3389/fphar.2022.1072715.
[67] T.T. Su, Drug screening in *Drosophila* ; why, when, and when not? WIREs Developmental Biology 8 (2019) https://doi.org/10.1002/wdev.346.

[68] K. Papanikolopoulou, A. Mudher, E. Skoulakis, An assessment of the translational relevance of Drosophila in drug discovery, Expert Opin Drug Discov 14 (2019) 303–313, https://doi.org/10.1080/17460441.2019.1569624.
[69] C. Munnik, M.P. Xaba, S.T. Malindisa, B.L. Russell, S.A. Sooklal, Drosophila melanogaster: a platform for anticancer drug discovery and personalized therapies, Front. Genet. 13 (2022), https://doi.org/10.3389/fgene.2022.949241.
[70] J.A. Tello, H.E. Williams, R.M. Eppler, M.L. Steinhilb, M. Khanna, Animal models of neurodegenerative disease: recent advances in fly highlight innovative approaches to drug discovery, Front. Mol. Neurosci. 15 (2022), https://doi.org/10.3389/fnmol.2022.883358.
[71] S.V. Nair, G. Baranwal, M. Chatterjee, A. Sachu, A.K. Vasudevan, C. Bose, A. Banerji, R. Biswas, Antimicrobial activity of plumbagin, a naturally occurring naphthoquinone from Plumbago rosea, against Staphylococcus aureus and Candida albicans, International Journal of Medical Microbiology 306 (2016) 237–248, https://doi.org/10.1016/j.ijmm.2016.05.004.
[72] T. de A. Hermes, A.B. Macedo, A.R. Fogaça, L.H.R. Moraes, F.M. de Faria, L. A. Kido, V.H.A. Cagnon, E. Minatel, Beneficial cilostazol therapeutic effects in *mdx* dystrophic skeletal muscle, Clin. Exp. Pharmacol. Physiol. 43 (2016) 259–267, https://doi.org/10.1111/1440-1681.12521.
[73] R.D. Mâncio, T. de A. Hermes, A.B. Macedo, D.S. Mizobuti, I.F. Rupcic, E. Minatel, Dystrophic phenotype improvement in the diaphragm muscle of mdx mice by diacerhein, PLoS One 12 (2017) e0182449, https://doi.org/10.1371/journal.pone.0182449.
[74] T. de A. Hermes, R.D. Mâncio, A.B. Macedo, D.S. Mizobuti, G.L. da Rocha, V.H. A. Cagnon, E. Minatel, Tempol treatment shows phenotype improvement in mdx mice, PLoS One 14 (2019) e0215590, https://doi.org/10.1371/journal.pone.0215590.
[75] N.P. Evans, J.A. Call, J. Bassaganya-Riera, J.L. Robertson, R.W. Grange, Green tea extract decreases muscle pathology and NF-κB immunostaining in regenerating muscle fibers of mdx mice, Clinical Nutrition 29 (2010) 391–398, https://doi.org/10.1016/j.clnu.2009.10.001.
[76] W. Sumsakul, T. Plengsuriyakarn, K. Na-Bangchang, Pharmacokinetics, toxicity, and cytochrome P450 modulatory activity of plumbagin, BMC Pharmacol Toxicol 17 (2016) 50, https://doi.org/10.1186/s40360-016-0094-5.
[77] N. Thakor, B. Janathia, Plumbagin: a potential candidate for future research and development, Curr Pharm Biotechnol 23 (2022) 1800–1812, https://doi.org/10.2174/1389201023666211230113146.
[78] J. Pei, X. Pan, G. Wei, Y. Hua, Research progress of glutathione peroxidase family (GPX) in redoxidation, Front. Pharmacol. 14 (2023), https://doi.org/10.3389/fphar.2023.1147414.
[79] A. Loboda, M. Damulewicz, E. Pyza, A. Jozkowicz, J. Dulak, Role of Nrf2/HO-1 system in development, oxidative stress response and diseases: an evolutionarily conserved mechanism, Cell. Mol. Life Sci. 73 (2016) 3221–3247, https://doi.org/10.1007/s00018-016-2223-0.
[80] V. Ngo, M.L. Duennwald, Nrf2 and oxidative stress: a general overview of mechanisms and implications in human disease, Antioxidants 11 (2022) 2345, https://doi.org/10.3390/antiox11122345.
[81] S. Kourakis, C.A. Timpani, J.B. de Haan, N. Gueven, D. Fischer, E. Rybalka, Targeting Nrf2 for the treatment of duchenne muscular dystrophy, Redox Biol. 38 (2021) 101803, https://doi.org/10.1016/j.redox.2020.101803.
[82] R. Sawicki, S.P. Singh, A.K. Mondal, H. Beneš, P. Zimniak, Cloning, expression and biochemical characterization of one Epsilon-class (GST-3) and ten Delta-class (GST-1) glutathione S-transferases from Drosophila melanogaster, and identification of additional nine members of the Epsilon class, Biochem. J. 370 (2003) 661–669, https://doi.org/10.1042/bj20021287.
[83] G.P. Sykiotis, D. Bohmann, Keap1/Nrf2 signaling regulates oxidative stress tolerance and lifespan in Drosophila, Dev. Cell 14 (2008) 76–85, https://doi.org/10.1016/j.devcel.2007.12.002.
[84] K. Pietraszek-Gremplewicz, M. Kozakowska, I. Bronisz-Budzynska, M. Ciesla, O. Mucha, P. Podkalicka, M. Madej, U. Glowniak, K. Szade, J. Stępniewski, M. Jez, K. Andrysiak, K. Bukowska-Strakova, A. Kaminska, A. Kostera-Pruszczyk, A. Józkowicz, A. Loboda, J. Dulak, Heme oxygenase-1 influences satellite cells and progression of duchenne muscular dystrophy in mice, Antioxid Redox Signal 29 (2018) 128–148, https://doi.org/10.1089/ars.2017.7435.
[85] S. Petrillo, L. Pelosi, F. Piemonte, L. Travaglini, L. Forcina, M. Catteruccia, S. Petrini, M. Verardo, A. D'Amico, A. Musarò, E. Bertini, Oxidative stress in Duchenne muscular dystrophy: focus on the NRF2 redox pathway, Hum. Mol. Genet. 26 (2017) 2781–2790, https://doi.org/10.1093/hmg/ddx173.
[86] J.T. Wangdi, M.F. O'Leary, V.G. Kelly, S.R. Jackman, J.C.Y. Tang, J. Dutton, J. L. Bowtell, Tart cherry supplement enhances skeletal muscle glutathione peroxidase expression and functional recovery after muscle damage, Med. Sci. Sports Exerc. 54 (2022) 609–621, https://doi.org/10.1249/MSS.0000000000002827.
[87] Q. Zhu, Y. Xiao, M. Jiang, X. Liu, Y. Cui, H. Hao, G.C. Flaker, Q. Liu, S. Zhou, Z. Liu, N-acetylcysteine attenuates atherosclerosis progression in aging LDL receptor deficient mice with preserved M2 macrophages and increased CD146, Atherosclerosis 357 (2022) 41–50, https://doi.org/10.1016/j.atherosclerosis.2022.08.008.
[88] Q. Zhu, S. Tai, L. Tang, Y. Xiao, J. Tang, Y. Chen, L. Shen, J. He, M. Ouyang, S. Zhou, N-acetyl cysteine ameliorates aortic fibrosis by promoting M2 macrophage polarization in aging mice, Redox Rep. 26 (2021) 170–175, https://doi.org/10.1080/13510002.2021.1976568.
[89] T. Yi, Z. Liu, H. Jia, Q. Liu, J. Peng, Sulforaphane regulates macrophage M1/M2 polarization to attenuate macrophage-induced caco-2 cell injury in an inflammatory environment, Iran J Immunol 21 (2024) 37–52, https://doi.org/10.22034/iji.2024.98644.2580.
[90] F. Chen, N. Guo, G. Cao, J. Zhou, Z. Yuan, Molecular analysis of curcumin-induced polarization of murine RAW264.7 macrophages, J. Cardiovasc. Pharmacol. 63 (2014) 544–552, https://doi.org/10.1097/FJC.0000000000000079.
[91] C. Xu, R. Guo, C. Hou, M. Ma, X. Dong, C. Ouyang, J. Wu, T. Huang, Resveratrol regulates macrophage recruitment and M1 macrophage polarization and prevents corneal allograft rejection in rats, Front. Med. 10 (2023), https://doi.org/10.3389/fmed.2023.1250914.
[92] C.-F. Tsai, G.-W. Chen, Y.-C. Chen, C.-K. Shen, D.-Y. Lu, L.-Y. Yang, J.-H. Chen, W.-L. Yeh, Regulatory effects of quercetin on M1/M2 macrophage polarization and oxidative/antioxidative balance, Nutrients 14 (2021) 67, https://doi.org/10.3390/nu14010067.
[93] A.M. Zaki, D.M. El-Tanbouly, R.M. Abdelsalam, H.F. Zaki, Plumbagin ameliorates hepatic ischemia-reperfusion injury in rats: role of high mobility group box 1 in inflammation, oxidative stress and apoptosis, Biomed. Pharmacother. 106 (2018) 785–793, https://doi.org/10.1016/j.biopha.2018.07.004.
[94] S.S. Messeha, N.O. Zarmouh, P. Mendonca, M.G. Kolta, K.F.A. Soliman, The attenuating effects of plumbagin on pro-inflammatory cytokine expression in LPS-activated BV-2 microglial cells, J. Neuroimmunol. 313 (2017) 129–137, https://doi.org/10.1016/j.jneuroim.2017.09.007.
[95] X. Zheng, C. Mao, H. Qiao, X. Zhang, L. Yu, T. Wang, E. Lu, Plumbagin suppresses chronic periodontitis in rats via down-regulation of TNF-α, IL-1β and IL-6 expression, Acta Pharmacol. Sin. 38 (2017) 1150–1160, https://doi.org/10.1038/aps.2017.19.
[96] O.S. Kwon, S.G. Noh, S.H. Park, R.H.I. Andtbacka, J.R. Hyngstrom, R. S. Richardson, Ageing and endothelium-mediated vascular dysfunction: the role of the NADPH oxidases, J Physiol 601 (2023) 451–467, https://doi.org/10.1113/JP283208.
[97] Z. Li, A. Chinnathambi, S. Ali Alharbi, F. Yin, Plumbagin protects the myocardial damage by modulating the cardiac biomarkers, antioxidants, and apoptosis signaling in the doxorubicin-induced cardiotoxicity in rats, Environ. Toxicol. 35 (2020) 1374–1385, https://doi.org/10.1002/tox.23002.
[98] J.P. Lefaucheur, C. Pastoret, A. Sebille, Phenotype of dystrophinopathy in old *MDX* mice, Anat. Rec. 242 (1995) 70–76, https://doi.org/10.1002/ar.1092420109.